

UNCLASSIFIED

AD NUMBER

ADB815791

LIMITATION CHANGES

TO:

Approved for public release; distribution is unlimited. Document partially illegible.

FROM:

Distribution authorized to U.S. Gov't. agencies and their contractors;
Administrative/Operational Use; 18 MAR 1946.
Other requests shall be referred to Office of Scientific Research and Development, Washington, DC 20301. Document partially illegible.

AUTHORITY

SOD memo dtd 2 Aug 1960

THIS PAGE IS UNCLASSIFIED

Reproduced by
AIR DOCUMENTS DIVISION



HEADQUARTERS AIR MATERIEL COMMAND
WRIGHT FIELD, DAYTON, OHIO

The
U.S. GOVERNMENT

IS ABSOLVED

FROM ANY LITIGATION WHICH MAY
ENSUE FROM THE CONTRACTORS IN-
FRINGING ON THE FOREIGN PATENT
RIGHTS WHICH MAY BE INVOLVED.

WRIGHT FIELD, DAYTON, OHIO

RFEL - C

4 8 5

A.T.I.

1 3 8 6 0

NDRC
Div. 14
ONR-262

Radiation Laboratory

Report 953

March 18, 1946

HYDROGEN THERMIONS IN PULSE GENERATOR CIRCUITS

Abstract

Data are presented on the operating characteristics of hydrogen thyratrons in line-type pulse generator circuits. Photographs of the rate of fall of anode voltage and rise of current at the start of conduction are shown, and graphs of voltage-current-power-impedance relationships permit calculation of energy dissipated per pulse. Data are presented to show that the ionization time depends directly on the gas pressure, and that tube drop depends directly on cathode emission for the ranges of pressure and emission covered by this work. In addition to the operating anode voltage and current, the most important parameter governing tube dissipation is gas pressure. This is demonstrated both calorimetrically and by V-I power plot. Because of the great number of possible variables that govern tube dissipation, most of them uncontrollable, it is impossible to reproduce data with any degree of accuracy.

S. J. Krulikoski, Jr.

Approved by:


Leader, Group 51

Title Page
Table of Contents
53 Numbered Pages


Head, Division 5

1-24525

TABLE OF CONTENTS

<u>Subject</u>	<u>Page</u>
I. Introduction	1
II. Rate of Fall of Anode Voltage, Rate of Rise of Anode Current, and Tube Drop	1
A. Effect of Gas Pressure on $\frac{deb}{dt}$ and $\frac{dib}{dt}$	1
B. Effect of Series Inductance and Shunt Capacity on $\frac{deb}{dt}$ and $\frac{dib}{dt}$	4
C. Thyatron $\frac{dib}{dt}$ Compared to $\frac{dv}{dt}$ of the Output Pulse on Resistance Load	4
D. Effect of Operating Power Level on $\frac{deb}{dt}$	16
III. Tube Drop	16
IV. Dissipation Measurements	
A. Power vs time for a single pulse and voltage-current-power-impedance relationships at start of conduction.	16
B. Average power dissipation versus pulse repetition frequency	32
C. Average power dissipation versus pulse duration.	32
D. Average power dissipation versus power level.	35
E. Average power dissipation as a function of pulse repetition frequency for constant duty.	35
F. Comparison of calorimetric data and V-I data for 1 usec. 1000/sec, and a 50 ohm circuit.	45

HYDROGEN THYRATRONS IN PULSE GENERATOR CIRCUITS

I. Introduction

Measurements of power dissipation, rate of fall of anode voltage ($\frac{deb}{dt}$), and rate of rise of anode current ($\frac{dib}{dt}$) in hydrogen thyratrons have been made to obtain more data on the operation of these tubes in line-type pulse generator circuits. Data were taken under a variety of conditions of pulse duration, pulse repetition frequency, and power level. The measurements were made on Sylvania 4C35 and 5C22 thyratrons, and the data on gas pressure and cathode emission were taken with the standard R.F. pressure gauge and peak emission tester used for testing hydrogen thyratrons. This report presents the data obtained from these measurements of ($\frac{deb}{dt}$), ($\frac{dib}{dt}$), and power dissipation.

No quantitative analysis has been made of these data, except to correlate the measurements with the observations of tubes running on life test.

II. Rate of Fall of Anode Voltage, Rate of Rise of Anode Current, and Tube Drop

Measurements of $\frac{deb}{dt}$, $\frac{dib}{dt}$, and tube drop, were made with the hydrogen thyatron operating as the switch in a line-type pulse generator circuit. Data on $\frac{deb}{dt}$ were taken by observing the anode voltage at the start of conduction with a 6 μ mf capacity divider and a synchroscope with a sweep speed of 10 inches per microsecond. Data on $\frac{dib}{dt}$ were taken by observing the current at the start of conduction through a non-inductive coaxial resistor in the cathode lead of the thyatron. Voltage-current time relationships were determined by using a commutating switch and observing both current and voltage simultaneously on the synchroscope. The tube drop was measured on a cathode ray tube whose vertical deflection plates were connected to the thyatron anode and cathode.

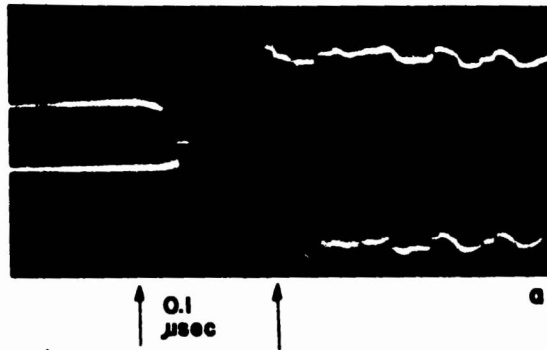
In the following discussion, ionization time is defined as the time taken for the anode voltage to fall from the maximum voltage before conduction to the flat region during conduction, as observed with a capacity divider and synchroscope.

A. Effect of Gas Pressure on $\frac{deb}{dt}$ and $\frac{dib}{dt}$

In Figure 1 and Figure 2 are shown $\frac{deb}{dt}$ and $\frac{dib}{dt}$ on two 4C35 tubes with different gas pressure, run in the same circuit under identical operating

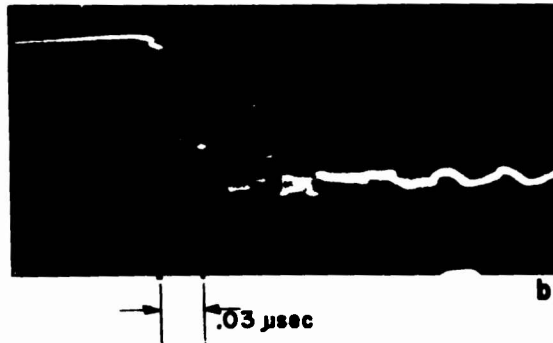
ANODE VOLTAGE - CURRENT - TIME RELATIONSHIPS AT
START OF 0.5 μ sec PULSE FOR 4C35 THYRATRON
(SYLVANIA -#5278 - 600 μ PRESSURE)

-2



FALL OF ANODE
VOLTAGE AND RISE
OF ANODE CURRENT

$e_b = 8.0$ KV
 $i_b = 90$ A
 $\tau = 0.5 \mu$ sec
 $\nu_r = 2000$ /sec
50 \sim CIRCUIT



FALL OF ANODE
VOLTAGE

$e_b = 8.0$ KV
TUBE DROP \sim 75 VOLTS

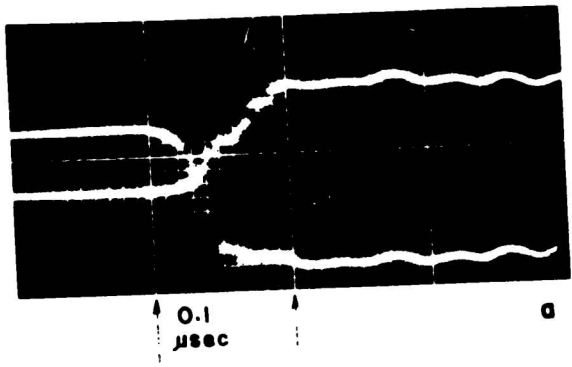


RISE OF ANODE
CURRENT

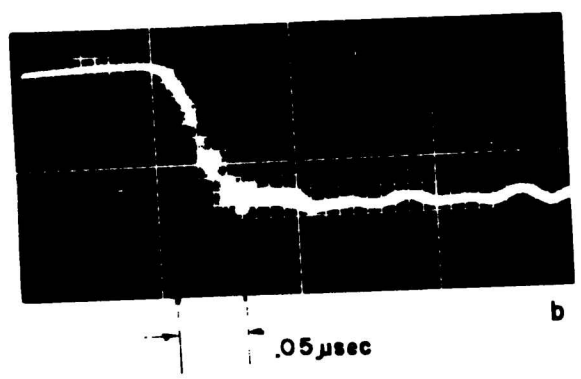
FIGURE 1

REPORT 953-2

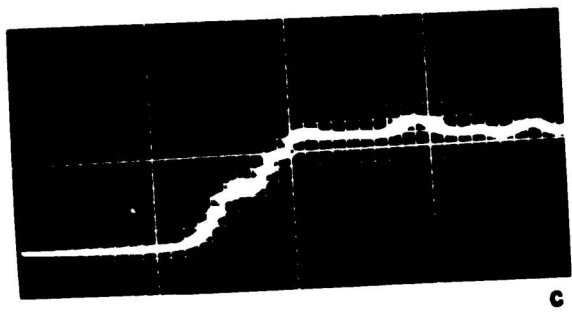
ANODE VOLTAGE - CURRENT - TIME RELATIONSHIPS AT
START OF 0.5 μ sec PULSE FOR 4C35 THYRATRON
(SYLVANIA - 48428 - 400 μ PRESSURE)



FALL OF ANODE
VOLTAGE AND RISE
OF ANODE CURRENT
 $e_b = 8.0$ K.V.
 $i_b = 90$ A
 $\tau = 0.5 \mu$ sec
 $\nu_r = 2000$ /sec
50- Ω CIRCUIT



FALL OF ANODE
VOLTAGE
 $e_b = 8.0$ K.V.
TUBE DROP \sim 80 VOLTS



RISE OF ANODE
CURRENT

FIGURE 2

conditions. In Figure 1b, the ionization time is about 05 μ sec for a gas pressure of 500 μ . In Figure 2b, for a gas pressure of 300 μ , the ionization time is about 05 μ sec. Comparing Figure 1b and Figure 2c, $\frac{dib}{dt}$ is higher for the higher pressure tube.

Figures 3, 4, and 5 show $\frac{deb}{dt}$ and $\frac{dib}{dt}$ on a 5C22 tube (pressure reading is 500 μ) for three different pulse lengths and repetition frequencies. In Figures 3b, 4b, and 5b, the ionization time is about the same, 05 μ sec, although Figures 3c, 4c, and 5c indicate that $\frac{dib}{dt}$ is slightly decreased as the pulse length is increased. This decrease in $\frac{dib}{dt}$ with increasing pulse length is due to the fact that type 5 networks of three to five sections were used, and the rate of rise of the pulse depends on the time delay per section of the network. In these particular cases, the time delay per section increased with the pulse length, and the rate of rise of the pulse was correspondingly reduced. Figures 6, 7, and 8 show data taken on a second 5C22 tube under the same operating conditions. This tube had a pressure reading of \approx 300 μ . Figures 6b, 7b, and 8b again show that the ionization time is approximately constant for different pulse lengths and repetition rates, although with the lower gas pressure, it is about 03 μ sec as compared to 05 μ sec for the 5C22 with higher gas pressure.

Figures 9 and 10 show 20 μ sec current pulses in five 4C35 tubes operated under identical circuit conditions. These data show that the rate of rise of thyatron current depends to a great extent on the tube as well as the circuit.

In Figures 9 and 10, $\frac{dib}{dt}$ increases with increasing gas pressure.

B. Effect of Series Inductance and Shunt Capacity on $\frac{deb}{dt}$ and $\frac{dib}{dt}$

Figure 11 shows the effect of the addition of 100 μ mf shunt capacity across the thyatron for a low pressure 5C22. (See Figures 6, 7, and 8.) The rate of fall of voltage is not appreciably affected, and the rate of rise of current is slightly increased.*

Figure 12 shows the effect of 5 μ h inductance in series with the anode lead for a high pressure thyatron. It is difficult to evaluate the effect of the inductance on $\frac{deb}{dt}$ because of the oscillations, but $\frac{dib}{dt}$ is greatly reduced.*

C. Thyatron $\frac{dib}{dt}$ compared to $\frac{dv}{dt}$ of the Output Pulse on Resistance Load

Figure 13 compares the thyatron current pulse and output voltage pulse on resistance load for two circuit conditions of increasing stray shunt

*See Radiation Laboratory Report 51-10/18/45, A Study of 5C22 Cathode Sparking in the Westinghouse SRA Modulator.

ANODE VOLTAGE - CURRENT - TIME RELATIONSHIPS AT START -5
 OF 0.25 μ sec PULSE FOR 5C22 THYRATRON
 (SYLVANIA - 54470 - 500 μ PRESSURE)

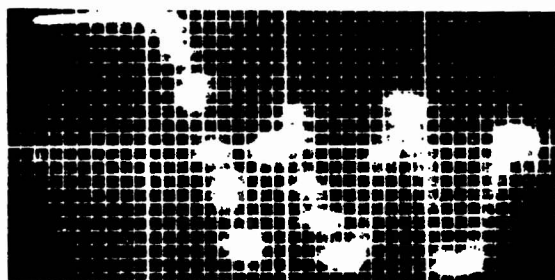


0.1 μ sec

a

FALL OF ANODE VOLTAGE
 AND RISE OF ANODE
 CURRENT

$e_b = 16.0$ K.V.
 $i_b = 144$ A
 $\tau = 0.25 \mu$ sec
 $\nu_r = 3000/\text{sec}$
 50 \sim CIRCUIT

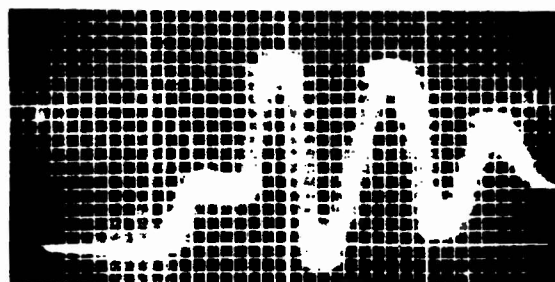


.05 μ sec

b

FALL OF ANODE
 VOLTAGE

$e_b = 16.0$ K.V.
 TUBE DROP ~ 120 VOLTS



c

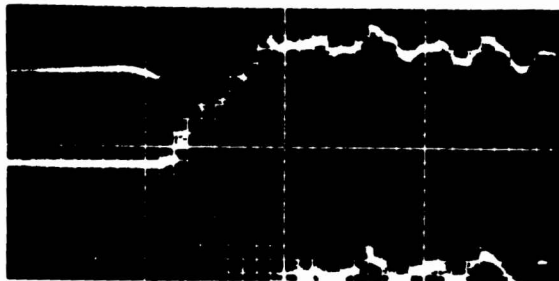
RISE OF ANODE
 CURRENT

FIGURE 3

REPORT 953-5

ANODE VOLTAGE - CURRENT - TIME RELATIONSHIPS AT
 START OF 0.5 usec PULSE FOR 5C22 THYRATRON
 (SYLVANIA - 54470 - 510 μ PRESSURE)

-6



FALL OF ANODE VOLTAGE
 AND RISE OF ANODE
 CURRENT

$e_b = 16.0$ K.V.
 $i_b = 144$ A
 $\tau = 0.5 \mu\text{sec}$
 $\nu = 2000/\text{sec}$
 50 \sim CIRCUIT

0.1
 μsec

a

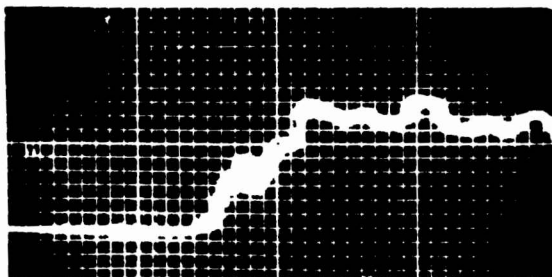


FALL OF ANODE VOLTAGE

$e_b = 16.0$ K.V.
 TUBE DROP ~ 120 VOLTS

0.06
 μsec

b



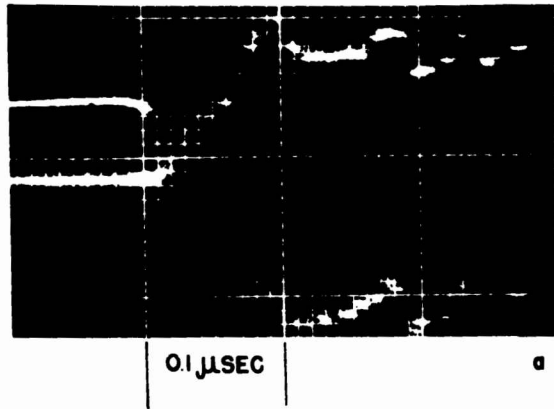
RISE OF ANODE CURRENT

c

FIGURE 4

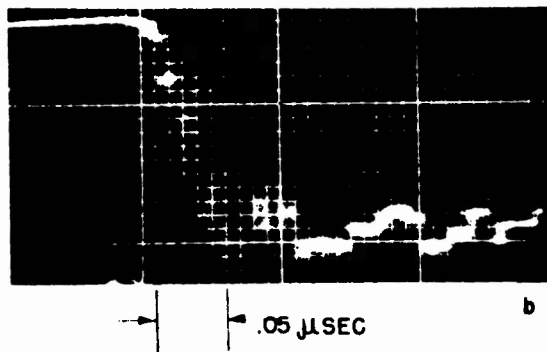
REPORT 953-6

ANODE VOLTAGE - CURRENT - TIME RELATIONSHIPS AT START
OF 1.1 μ SEC PULSE FOR 5C22 THYRATRON
(SYLVANIA - 54470 - 500 μ PRESSURE)



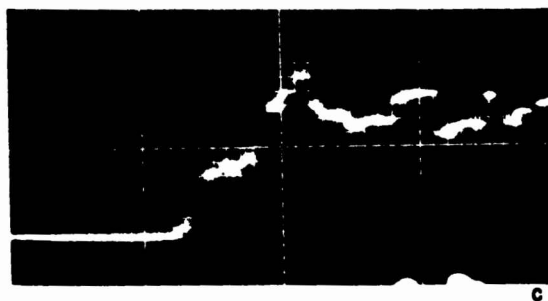
FALL OF ANODE VOLTAGE
AND RISE OF CURRENT

$e_b = 16.0$ KV
 $i_b = 144$ A
 $\tau = 1.1$ μ SEC
 $V_r = 1000$ /SEC
50 Ω CIRCUIT



FALL OF ANODE VOLTAGE

$e_b = 16.0$ KV
TUBE DROP ~ 120 V

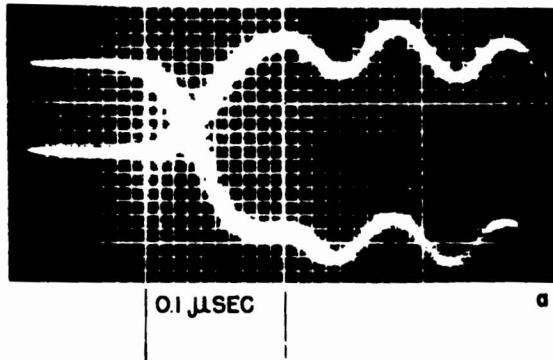


RISE OF ANODE CURRENT

FIGURE 5

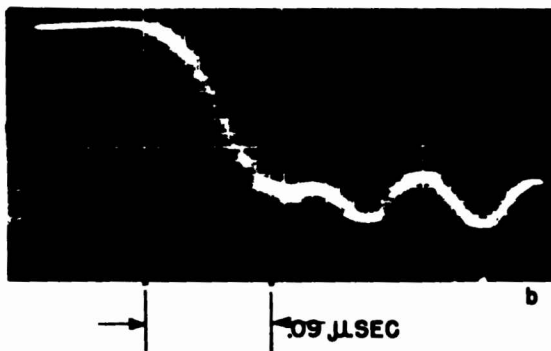
REPORT 953-7

ANODE VOLTAGE - CURRENT - TIME RELATIONSHIPS AT START
 OF 0.25 μ SEC PULSE FOR 5C22 THYRATRON
 (SYLVANIA - 57502 - $\approx 300\mu$ PRESSURE)



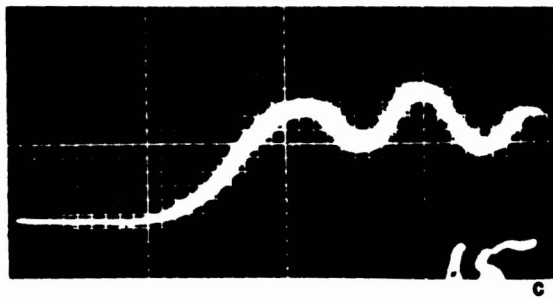
FALL OF ANODE VOLTAGE
 AND RISE OF ANODE CURRENT

$e_b = 16.0$ KV
 $i_b = 144$ A
 $\tau = 0.25$ μ SEC
 $V_r = 3000$ /SEC
 50Ω CIRCUIT



FALL OF ANODE VOLTAGE

$e_b = 16.0$ KV
 TUBE DROP ~ 125 VOLTS

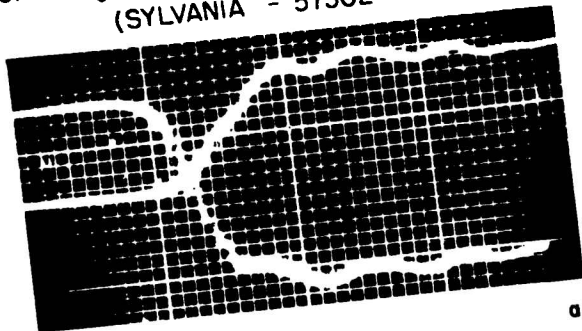


RISE OF ANODE CURRENT

FIGURE 6

REPORT 953-8

ANODE VOLTAGE - CURRENT - TIME RELATIONSHIPS AT START
 OF 0.5 μSECOND PULSE FOR 5C22 THYRATRON
 (SYLVANIA - 57502 - 300 μ PRESSURE)

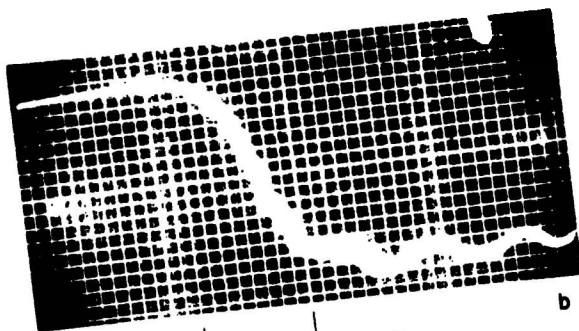


FALL OF ANODE VOLTAGE
 AND RISE OF ANODE
 CURRENT

$e_b = 16.0 \text{ KV}$
 $i_b = 144 \text{ A}$
 $\tau = 0.5 \mu\text{SEC}$
 $V_r = 2000/\text{SEC}$
 $50 \Omega \text{ CIRCUIT}$

01 μSEC

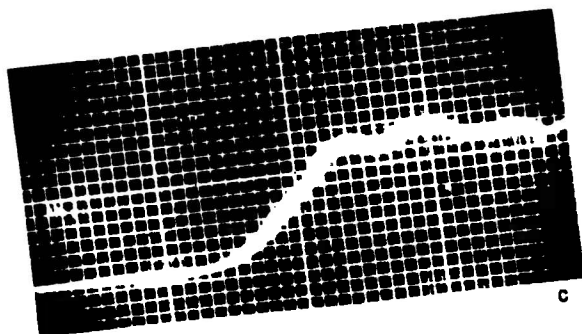
a



FALL OF ANODE VOLTAGE
 $e_b = 16.0 \text{ KV}$
 TUBE DROP ~125VOLTS

.08 μSEC

b

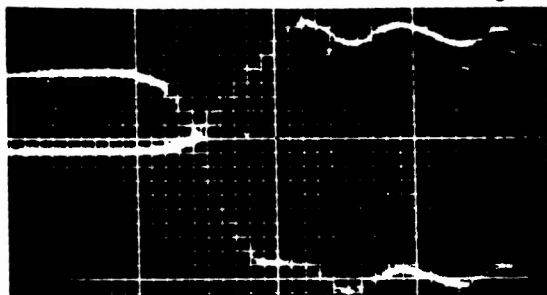


RISE OF ANODE CURRENT

c

FIGURE 7

ANODE VOLTAGE - CURRENT - TIME RELATIONSHIPS AT START
 OF 1.1 USEC PULSE FOR 5C22 THYRATRON
 (SYLVANIA - 57502 - 300 μ PRESSURE)

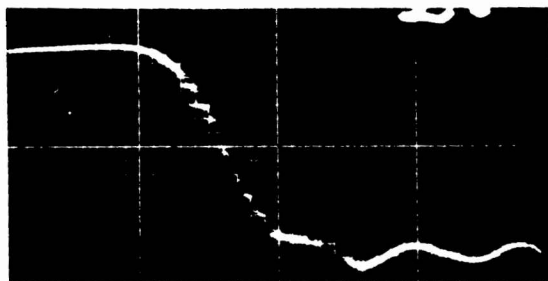


0.1 μ SEC

a

FALL OF ANODE VOLTAGE
 AND RISE OF ANODE CURRENT

$e_b = 16.0$ KV
 $i_b = 14.4$ A
 $\tau = 1.1$ μ SEC
 $V_r = 1000$ /SEC
 50Ω CIRCUIT

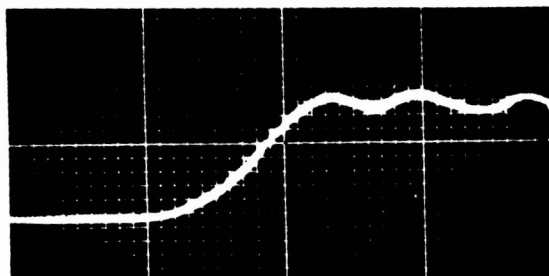


→ ← .10 μ SEC

b

FALL OF ANODE VOLTAGE

$e_b = 16.0$ KV
 TUBE DROP ~ 125 VOLTS



c

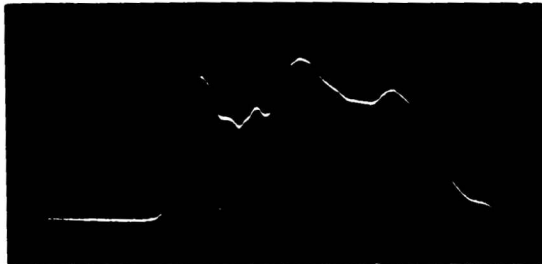
FIGURE 8

REPORT 953-10



48428
 380 MICRONS PRESSURE
 61 VOLT EMISSION DROP
 AT 90A

a



461974
 450 MICRONS PRESSURE
 50 VOLT EMISSION DROP
 AT 90A

b



5278
 650 MICRONS PRESSURE
 50 VOLT EMISSION DROP
 AT 90A

c

4C35 THYRATRON CURRENT PULSE SHAPE AS A FUNCTION
 OF GAS PRESSURE

$e_b = 8.0 \text{ KV}$
 $i_b = \sim 90 \text{ A}$
 $\tau = 0.25 \mu\text{SEC}$
 $V_r = 1000/\text{SEC}$

FIGURE 9



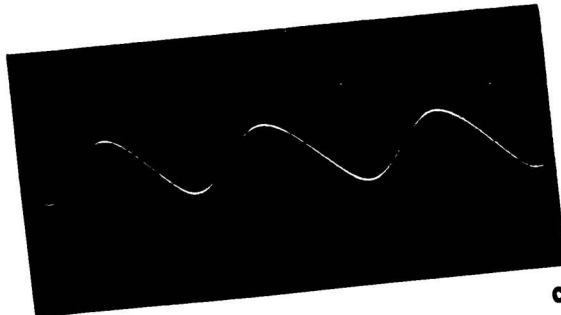
52341
 680 MICRONS PRESSURE
 130 VOLT EMISSION
 DROP AT 90A

a



52558
 820 MICRONS PRESSURE
 66 VOLT EMISSION
 DROP AT 90A

b



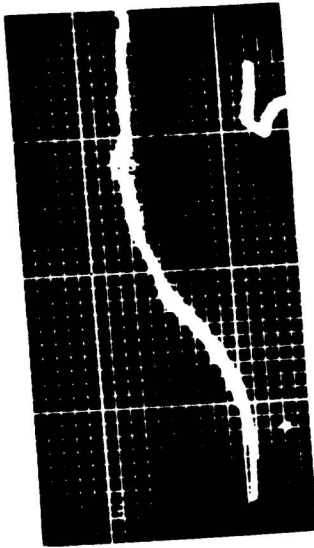
5 MC
 SWEEP CALIBRATION
 SIGNAL

c

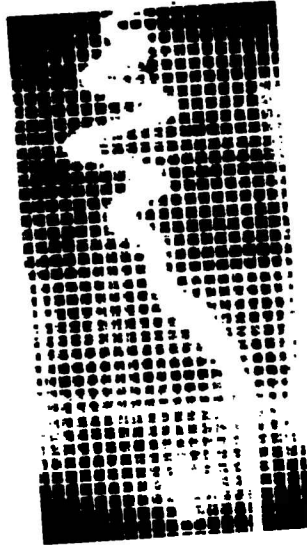
4C35 THYRATRON CURRENT PULSE SHAPE AS A
 FUNCTION OF GAS PRESSURE

$e_b = 8.0 \text{ K.V.}$
 $i_b = \sim 90 \text{ A}$
 $\tau = 0.25 \mu\text{sec}$
 $\omega_r = 1000/\text{sec}$

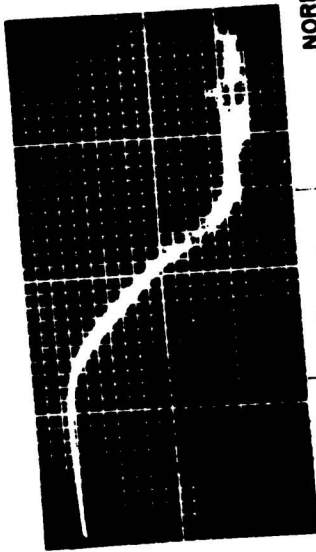
FIGURE 10



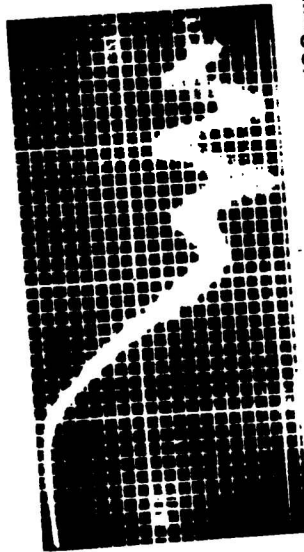
RISE OF CURRENT



RISE OF CURRENT



FALL OF VOLTAGE
0.14 μ sec



FALL OF VOLTAGE

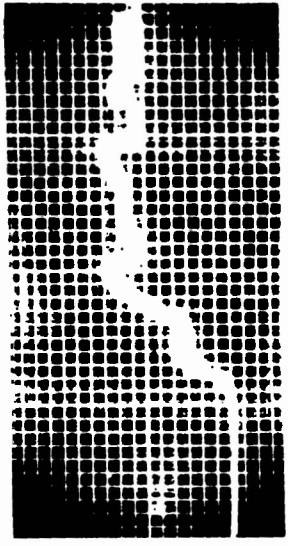
100 μ f ACROSS THYRATRON

RISE OF CURRENT ON $\frac{di_b}{dt}$ AND $\frac{dv_b}{dt}$

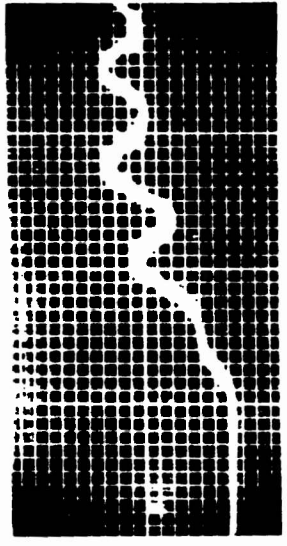
EFFECT OF SHUNT CAPACITY ACROSS THYRATRON ON $\frac{di_b}{dt}$ AND $\frac{dv_b}{dt}$
 $\tau = 0.5 \mu$ sec
 $e_b = 16.0$ K.V.
 $i_b = 14.4$ A
 $V_p = 1000$ /sec

(SYLVANIA 5C22 - 57502 - 300 μ PRESSURE)

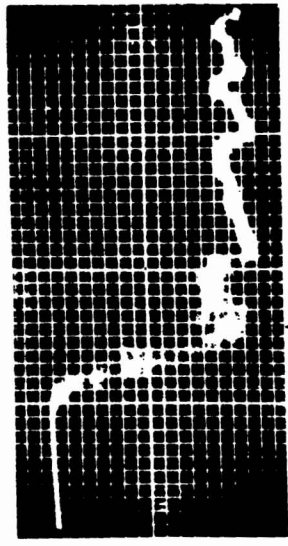
FIGURE 11



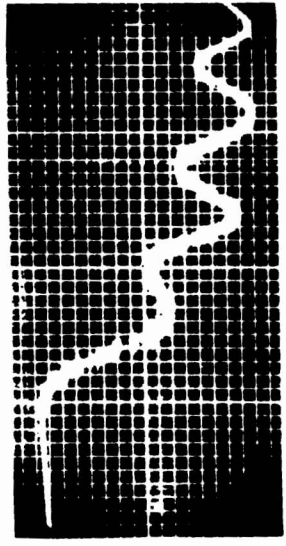
RISE OF CURRENT



RISE OF CURRENT



FALL OF VOLTAGE
0.05 μ SEC



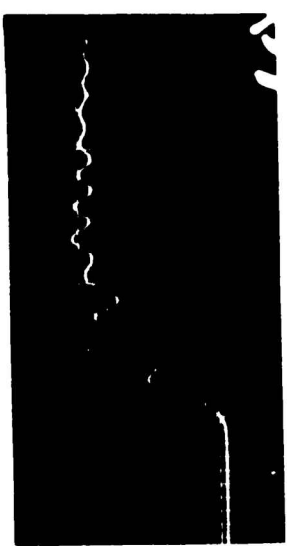
FALL OF VOLTAGE
EFFECT ON $\frac{dv}{dt}$ AND $\frac{di}{dt}$ OF ANODE INDUCTANCE IN SERIES WITH THYRATRON

5 μ h SERIES L

$v_b = 16.0$ KV $\tau = 0.5 \mu$ SEC
 $i_b = 144$ A $V_f = 1000$ / SEC

(SYLVANIA 5C22 - 57511 - 600 μ PRESSURE)

FIGURE 12

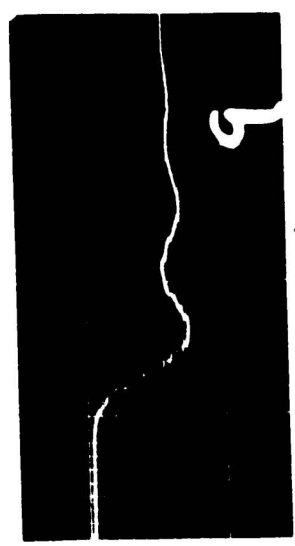


NORMAL CIRCUIT
THYRATRON CURRENT

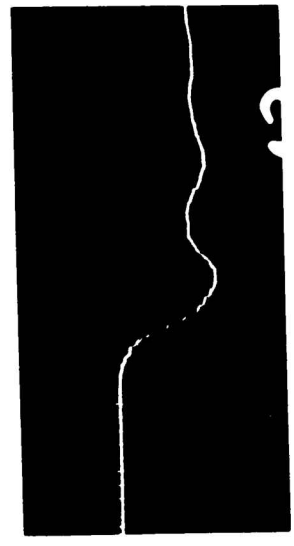


100 μ f ACROSS THYRATRON
THYRATRON CURRENT

$e_b = 16.0 \text{ KV}$ $\tau = 1.1 \mu\text{SEC}$
 $i_b = 170 \text{ A}$ $V_f = 1000 / \text{SEC}$



0.2 μ SEC
OUTPUT VOLTAGE ON R-LOAD



100 μ f ACROSS THYRATRON
OUTPUT VOLTAGE ON R-LOAD
COMPARISON OF 5C22 CURRENT PULSE AND OUTPUT VOLTAGE PULSE

FIGURE 13

capacity across the cathode circuit in the case of a hydrogen thyatron.

These data show that $\frac{dib}{dt}$ on the thyatron is greater than would be expected

from the network because of the stray shunt capacity across the thyatron. This stray capacity, charged to full switch voltage, is discharged through the thyatron, and all the energy is dissipated in the thyatron. It is evident in Figure 21 that the discharge current of this capacity does not

appear at the load*. For this reason, measurements of thyatron $\frac{dib}{dt}$ should be made at the thyatron and not on the load voltage pulse.

D. Effect of Operating Power Level on $\frac{deb}{dt}$

Figures 14, 15, and 16 show $\frac{deb}{dt}$ and $\frac{dib}{dt}$ on a 4C35 operated in a 50 ohm circuit with anode voltages of 5.0, 7.0, and 2.0 kv. Of necessity, $\frac{deb}{dt}$ varies with the anode voltage, but the ionization time is the same for all three operating points.

III. Tube Drop

In Figure 17 is shown the anode-cathode tube drop for a 4C35 operated at 1.1 usec pulse duration, and increasing peak current in a 50 ohm circuit. For this tube, the anode-cathode tube drop is nearly constant for increasing peak current.

In Figure 18 is shown the anode-cathode tube drop on two 4C35 tubes, operated under identical conditions of 1.1 usec pulse duration, but with different values of measured cathode emission. In these two tubes with approximately equal gas pressure, the tube drop varies directly with the emission drop.

Figures 19 and 20 compare the tube drop on three 4C35 tubes with the emission drop as measured with the standard thyatron peak emission tester. These data show that the anode-cathode tube drop can be approximately determined from the measured cathode emission.

Figure 21 shows the anode-cathode tube drop on three 5022 tubes.

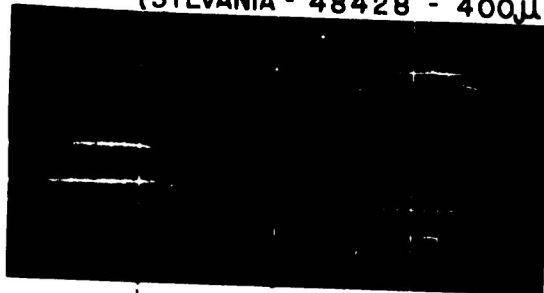
IV. Dissipation Measurements

A. Power vs time for a single pulse and voltage-current-power-impedance relationships at start of conduction

Figures 22 - 28 show graphs of power vs time for a single pulse, and voltage-current-power-impedance relationships at the start of conduction

*See Radiation Laboratory Report 828, Pages 14-17.

ANODE VOLTAGE - CURRENT - TIME RELATIONSHIPS AT START
 OF 1.1 μ SEC PULSE FOR 4C35 THYRATRON
 (SYLVANIA - 48428 - 400 μ PRESSURE)



0.1 μ SEC

FALL OF ANODE VOLTAGE
 AND RISE OF ANODE CURRENT

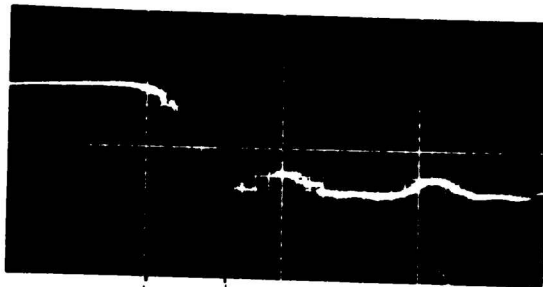
$e_b = 8.0$ KV

$I_b = 85$ A

$T = 1.1$ μ SEC

$V_r = 1000$ /SEC

50 Ω CIRCUIT

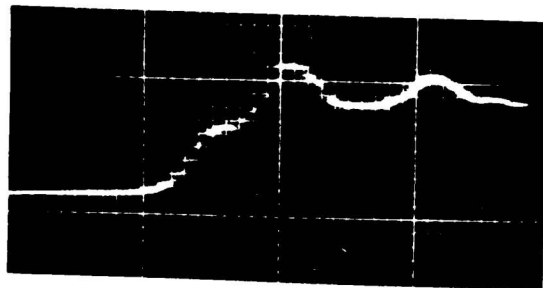


.06 μ SEC

FALL OF ANODE VOLTAGE

$e_b = 8.0$ KV

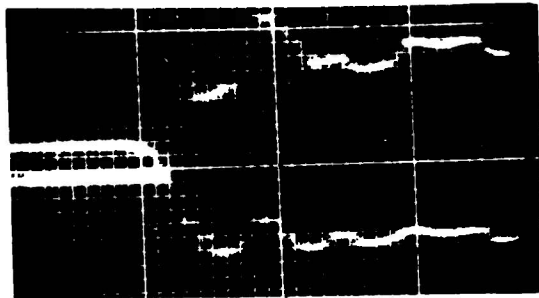
TUBE DROP ~ 80 V



RISE OF ANODE CURRENT

FIGURE 14

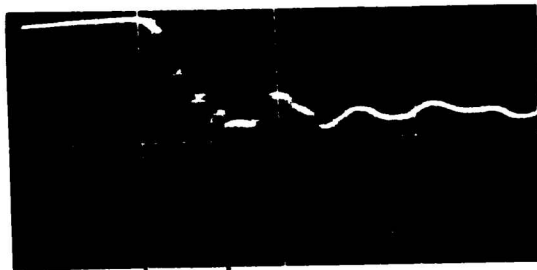
ANODE VOLTAGE - CURRENT - TIME RELATIONSHIPS AT START OF 1.0 μ SEC
 PULSE FOR 4C35 THYRATRON
 (SYLVANIA - 48428 - 400 μ PRESSURE)



FALL OF ANODE VOLTAGE AND
 RISE OF ANODE CURRENT

$e_b = 4.0 \text{ KV}$
 $i_b = 38 \text{ A}$
 $\tau = 1.0 \mu\text{SEC}$
 $V_T = 1000/\text{SEC}$
 $50 \Omega \text{ CIRCUIT}$

0.1 μ SEC



FALL OF ANODE VOLTAGE

$e_b = 4.0 \text{ KV}$
 TUBE DROP $\sim 75 \text{ V}$

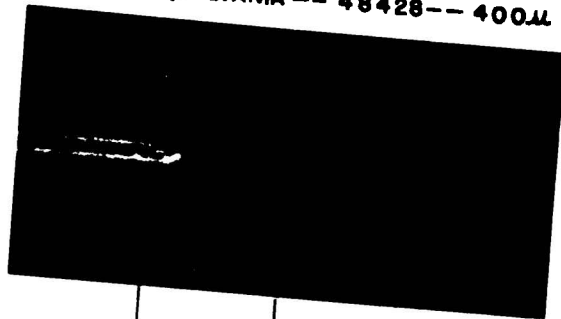
0.06 μ SEC



RISE OF ANODE CURRENT

FIGURE 15

ANODE VOLTAGE - CURRENT - TIME RELATIONSHIPS AT START OF
1.1 μ SEC PULSE FOR 4C35 THYRATRON
(SYLVANIA -- 48428 -- 400 μ PRESSURE)



→ 0.1 μ SEC ←

FALL OF ANODE VOLTAGE AND
RISE OF ANODE CURRENT

$E_b = 2.0 \text{ KV}$
 $i_b = 17 \text{ A}$
 $T = 1.1 \mu \text{ SEC}$
 $V_r = 1000 / \text{SEC}$
50 Ω CIRCUIT



→ .06 μ SEC ←

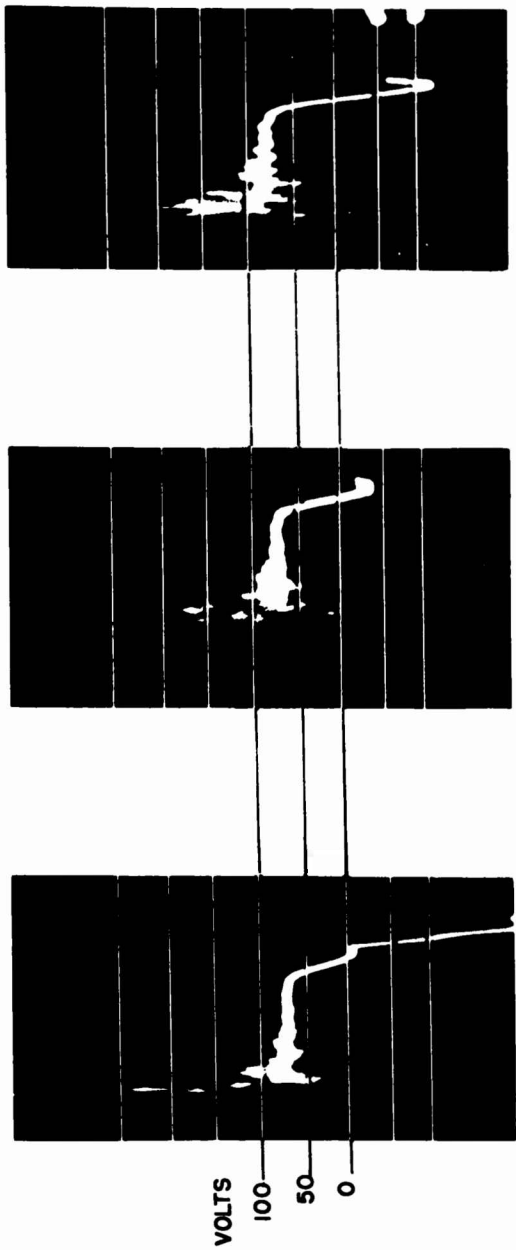
FALL OF ANODE VOLTAGE

$E_b = 2.0 \text{ KV}$
TUBE DROP ≈ 75 VOLTS



RISE OF ANODE CURRENT

FIGURE 16



TUBE DROP ~80V
 eb = 8.0KV
 ib ~85A

TUBE DROP ~75VOLTS
 eb = 4.0KV
 ib ~38A

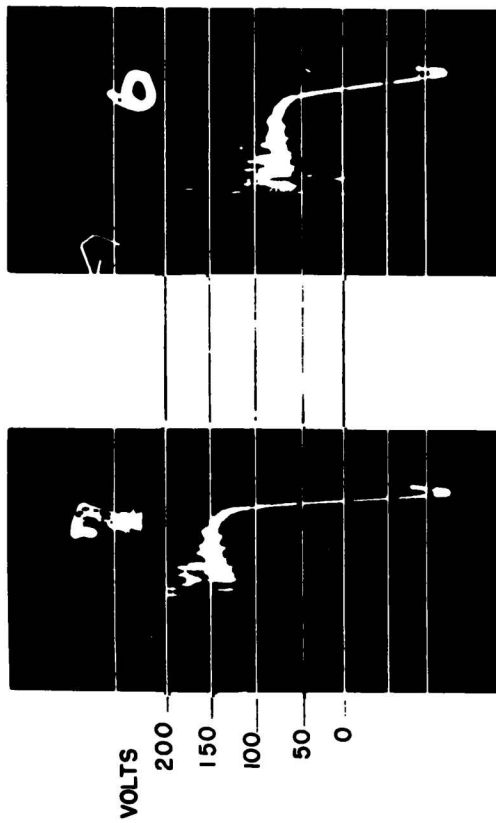
TUBE DROP ~75 V
 eb = 2.0KV
 ib ~17A

$\tau = 1.1 \mu\text{SEC}$
 $V_r = 1000/\text{SEC}$
 50 Ω CIRCUIT

ANODE - CATHODE VOLTAGE DROP DURING PULSE FOR 4C35 HYDROGEN
 THYRATRON
 (SYLVANIA -48428 - 400 μ PRESSURE)

FIGURE 17

ANODE-CATHODE VOLTAGE DROP DURING PULSE FOR 4C35 HYDROGEN THYRATRONS



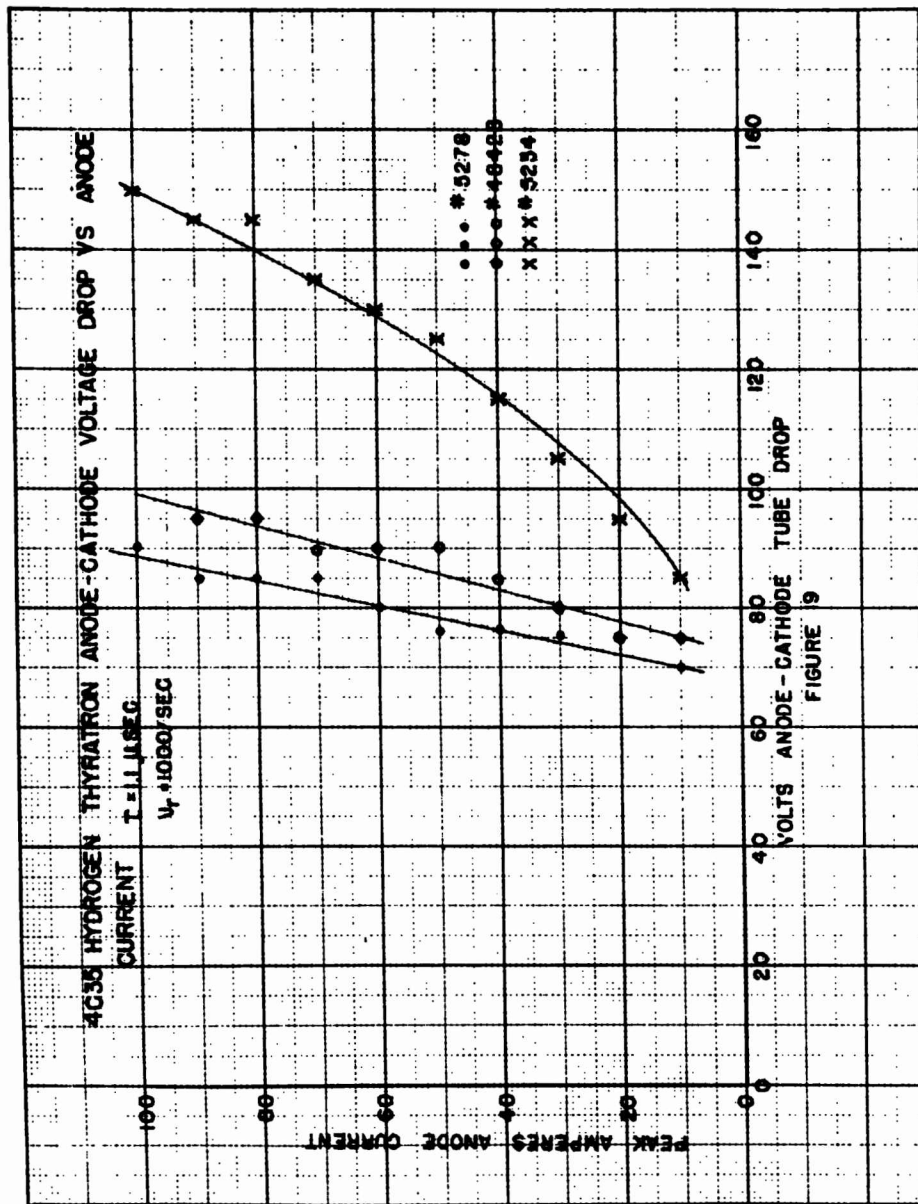
52341

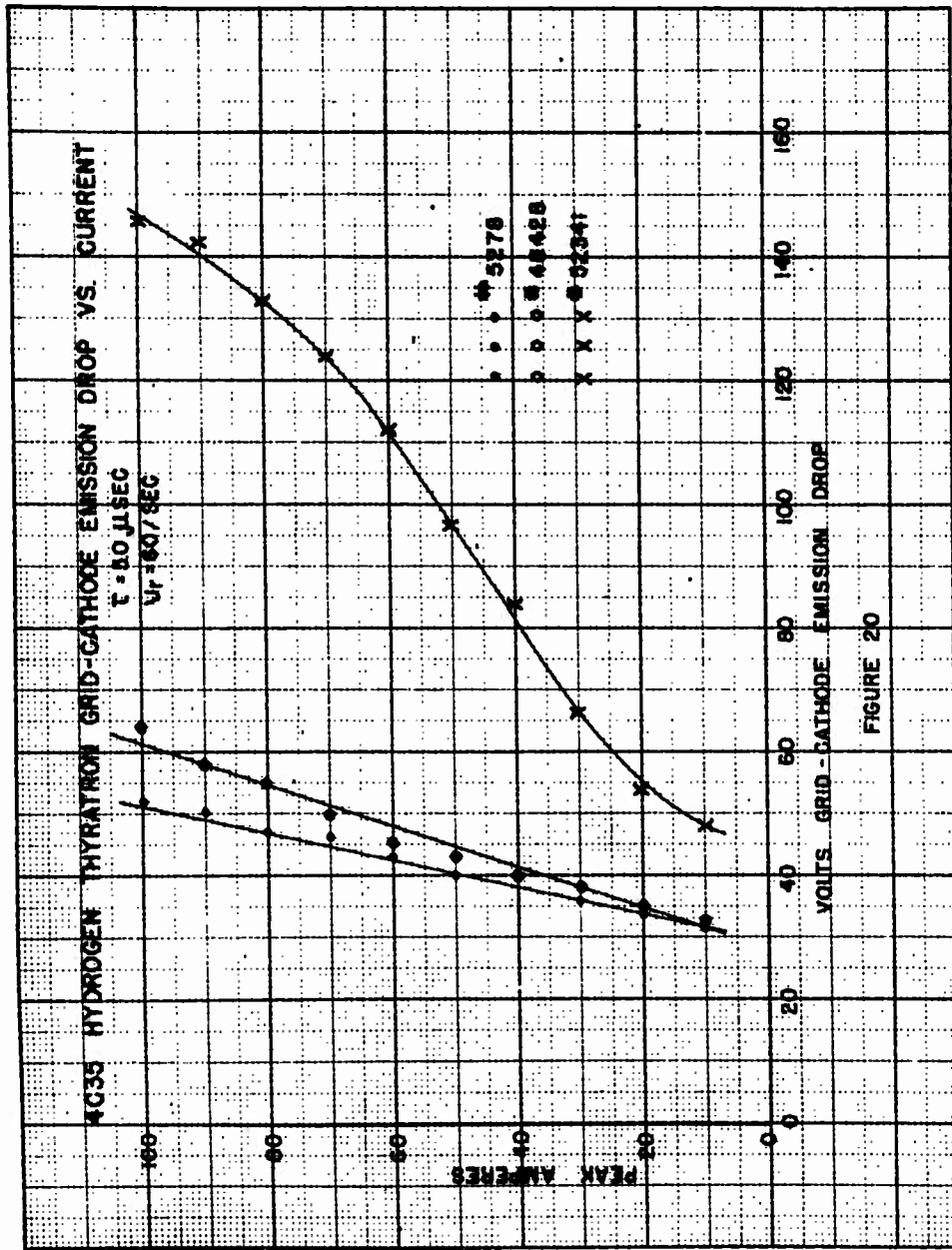
5278

TUBE DROP ~ 150 VOLTS
 EMISSION DROP = 130 VOLTS
 AT 90 A
 GAS PRESSURE = 680 μ
 $e_b = 80 \text{ KV}$
 $i_b = \sim 90 \text{ A}$
 $\tau = 1.1 \mu\text{SEC}$
 $V_r = 1000/\text{SEC}$

TUBE DROP ~ 75 VOLTS
 EMISSION DROP = 50 VOLTS
 AT 90 A
 GAS PRESSURE = 650 μ
 $e_b = 80 \text{ KV}$
 $i_b = \sim 90 \text{ A}$
 $\tau = 1.1 \mu\text{SEC}$
 $V_r = 1000/\text{SEC}$

FIGURE 18





ANODE - CATHODE VOLTAGE DROP DURING PULSE FOR 5C22 HYDROGEN THYRATRON

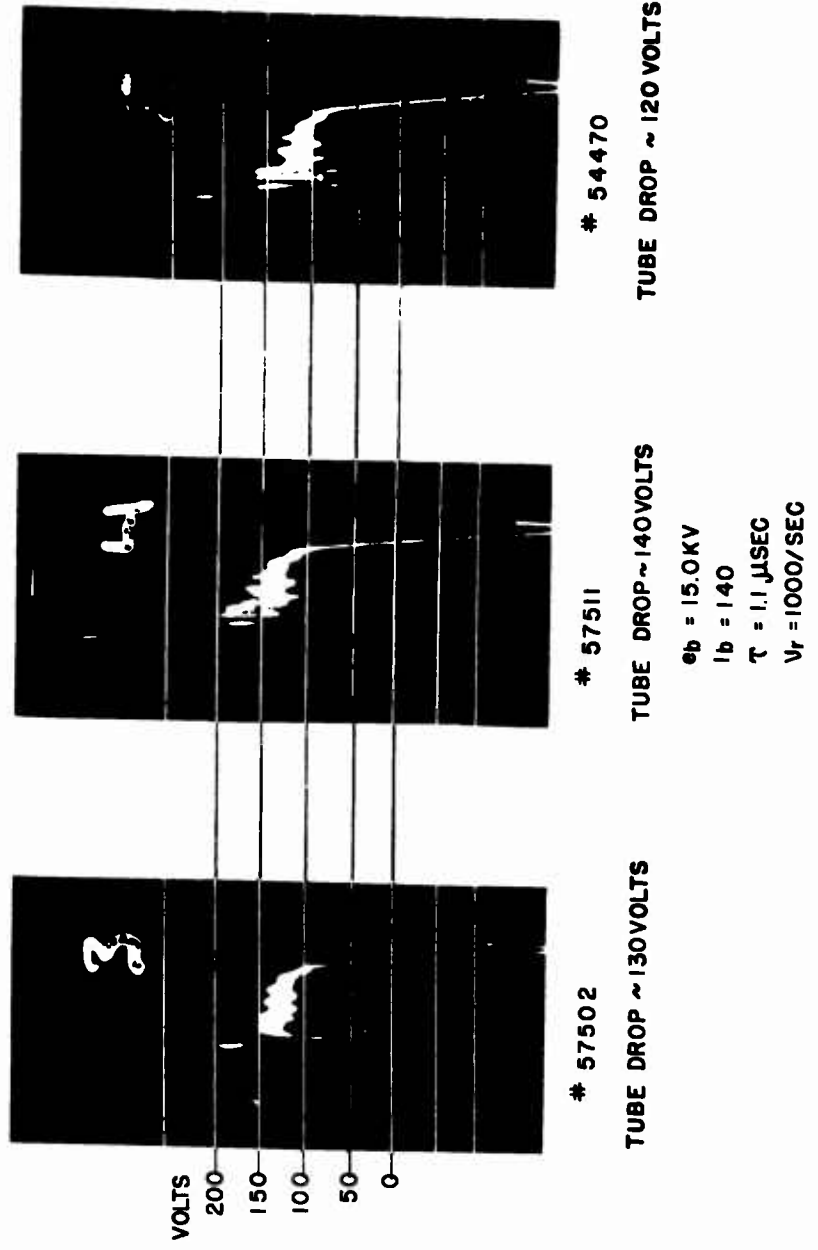


FIGURE 21

POWER VS. TIME FOR 11 J1SEC. PULSE

SYLVANIA 4C35

#52341 (600 μ A)

$e_b = 8KV$

$i_b = 85A$

$T = 11 \mu$ SEC

$V_f = 100V/SEC$

50 Ω CIRCUIT

1.9×10^{-3} JOULES PER PULSE

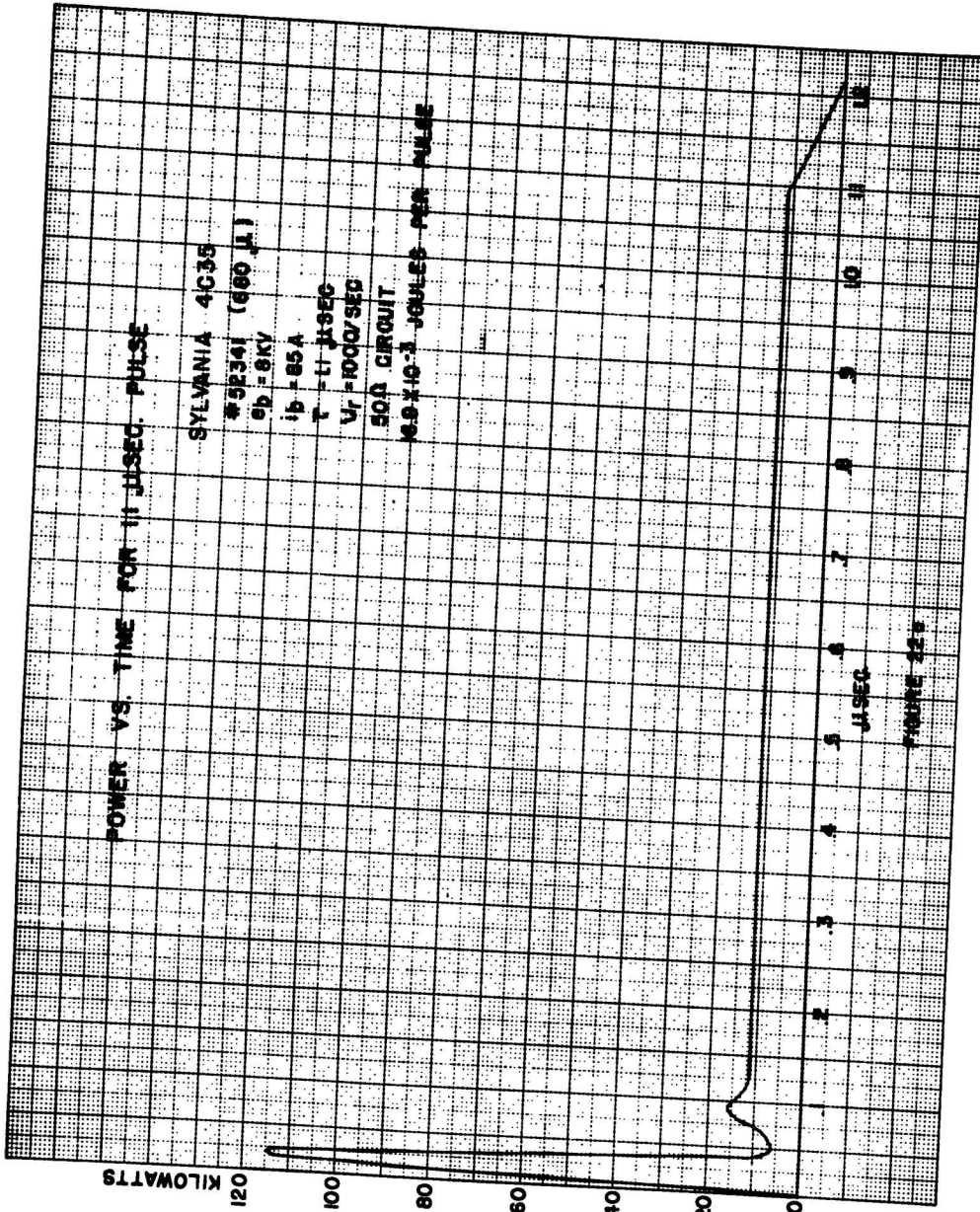


FIGURE 22

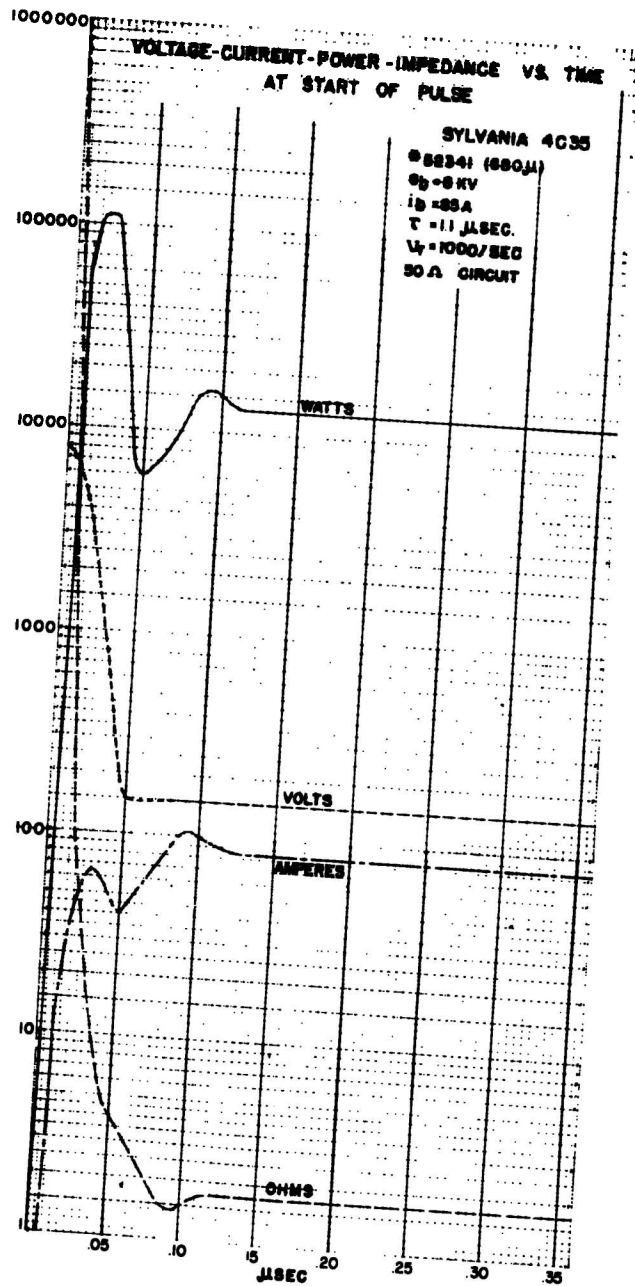
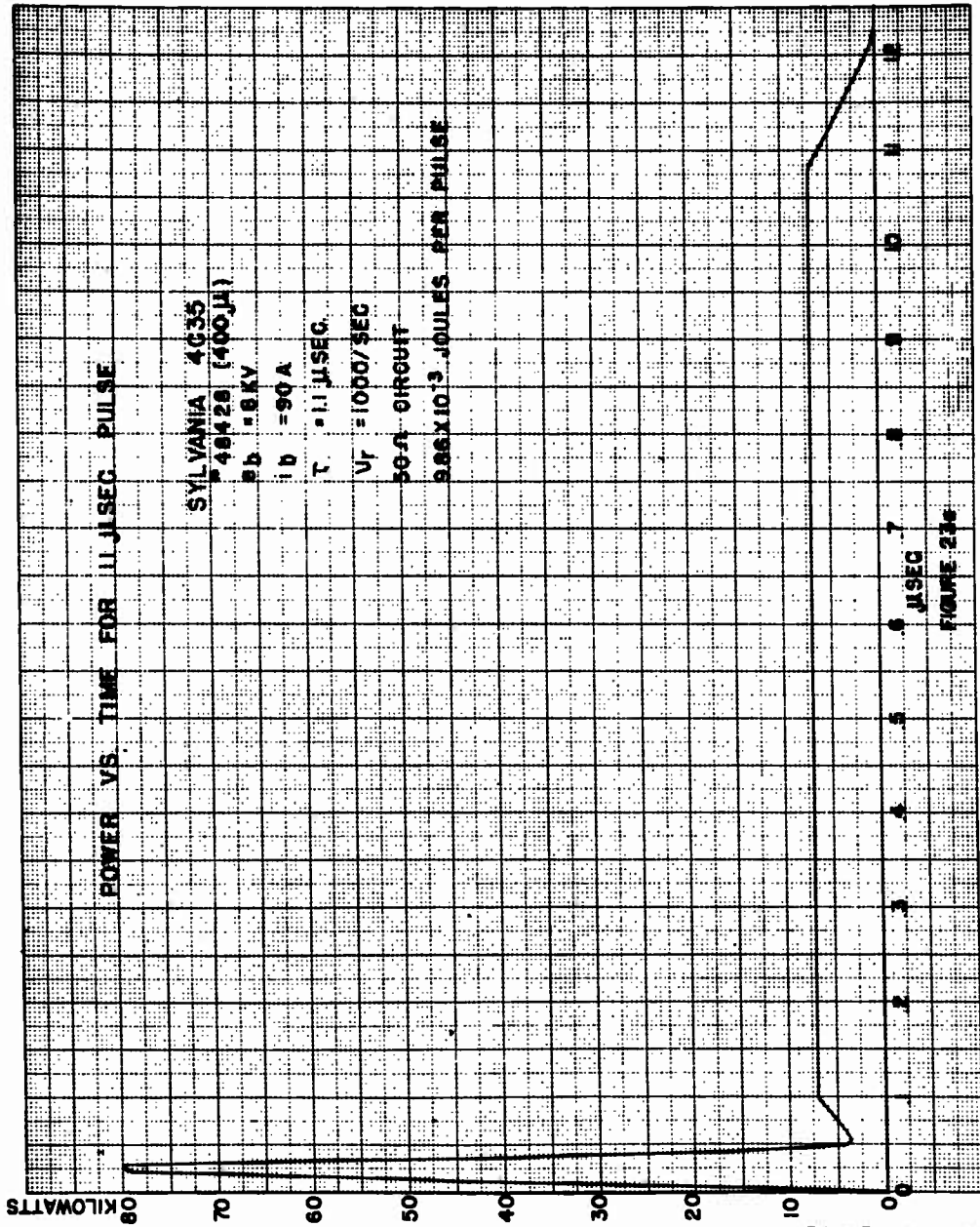


FIGURE 22 b



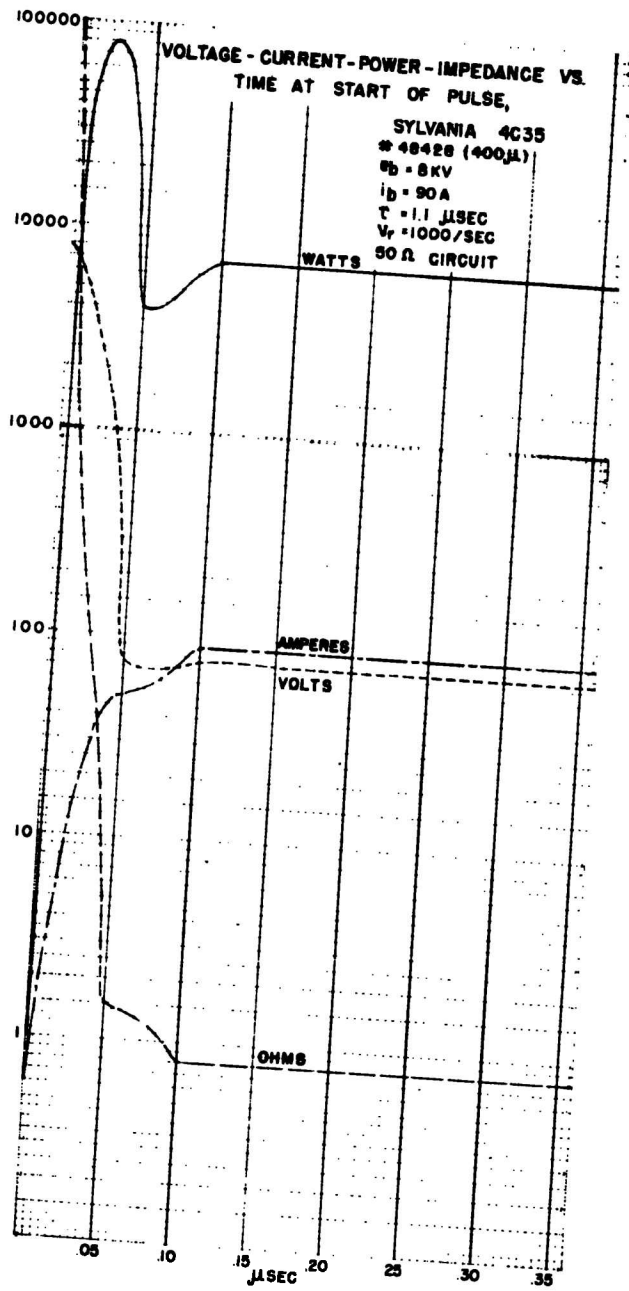
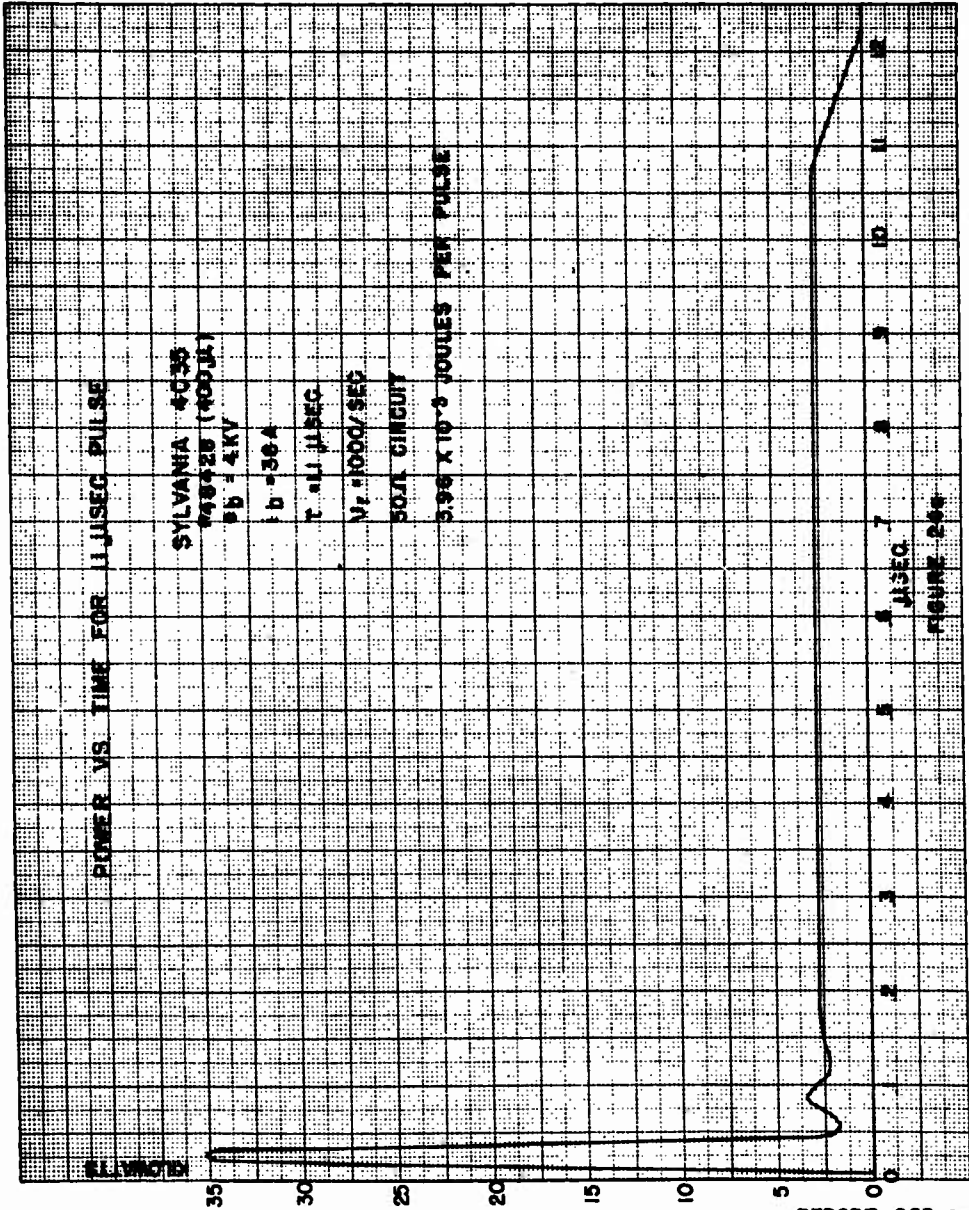


FIGURE 23b



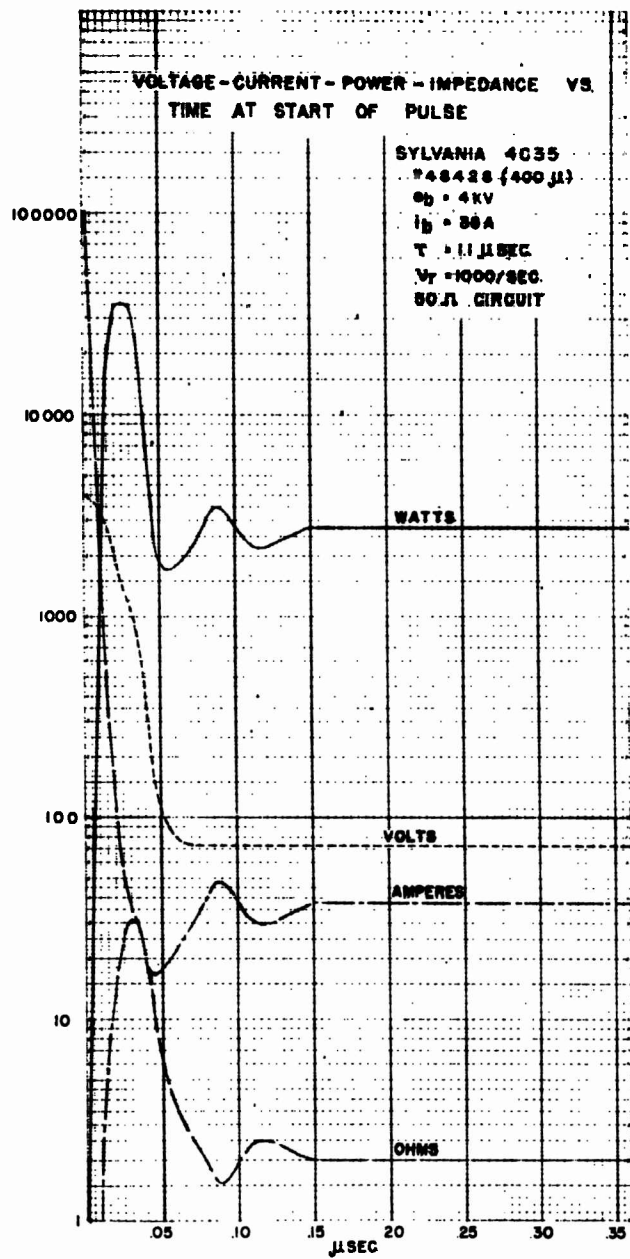


FIGURE 24b



FIGURE 25c

VOLTAGE - CURRENT - POWER - IMPEDANCE VS TIME
AT START OF PULSE

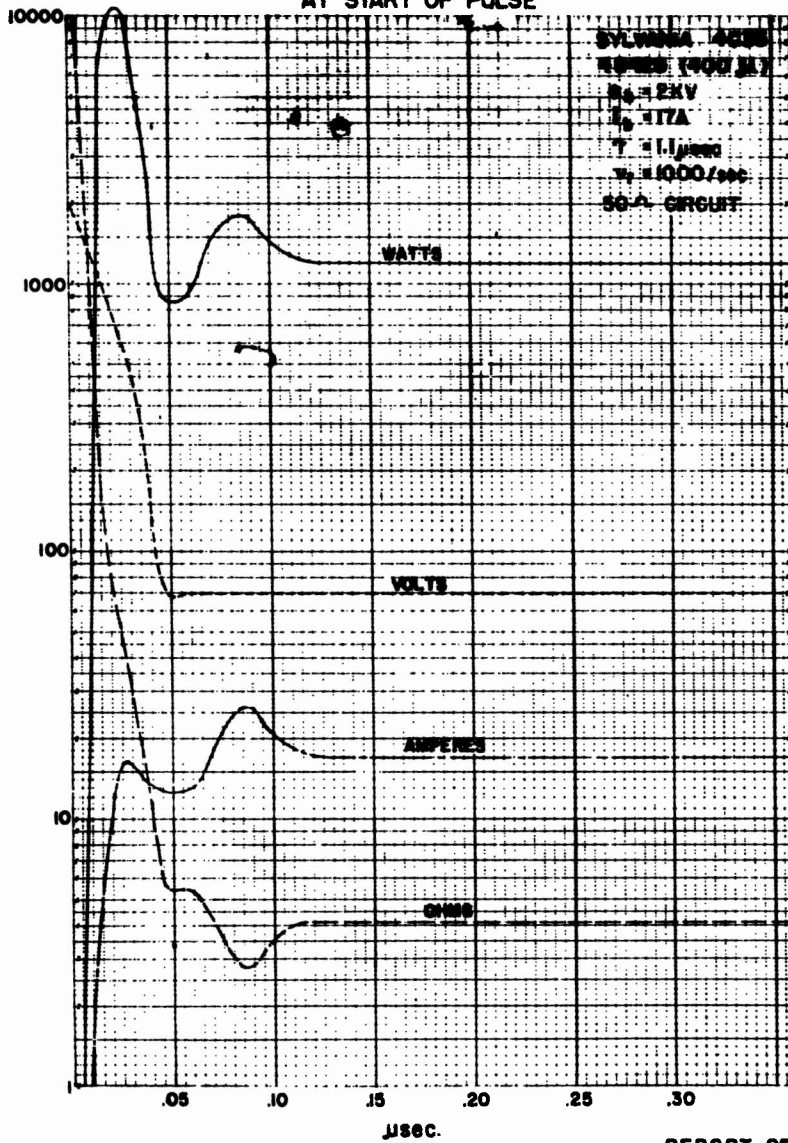
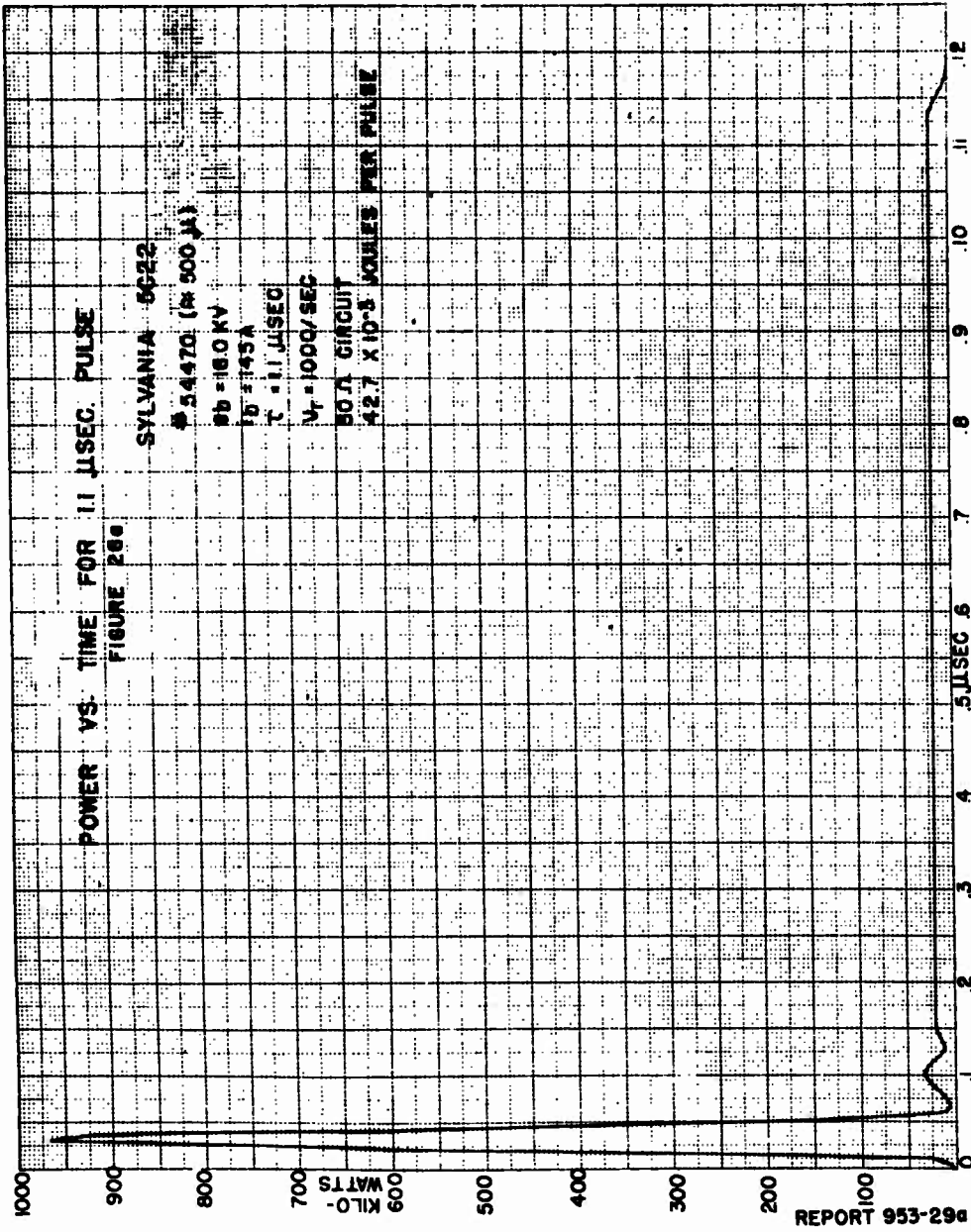


FIGURE 25b

REPORT 953-28b



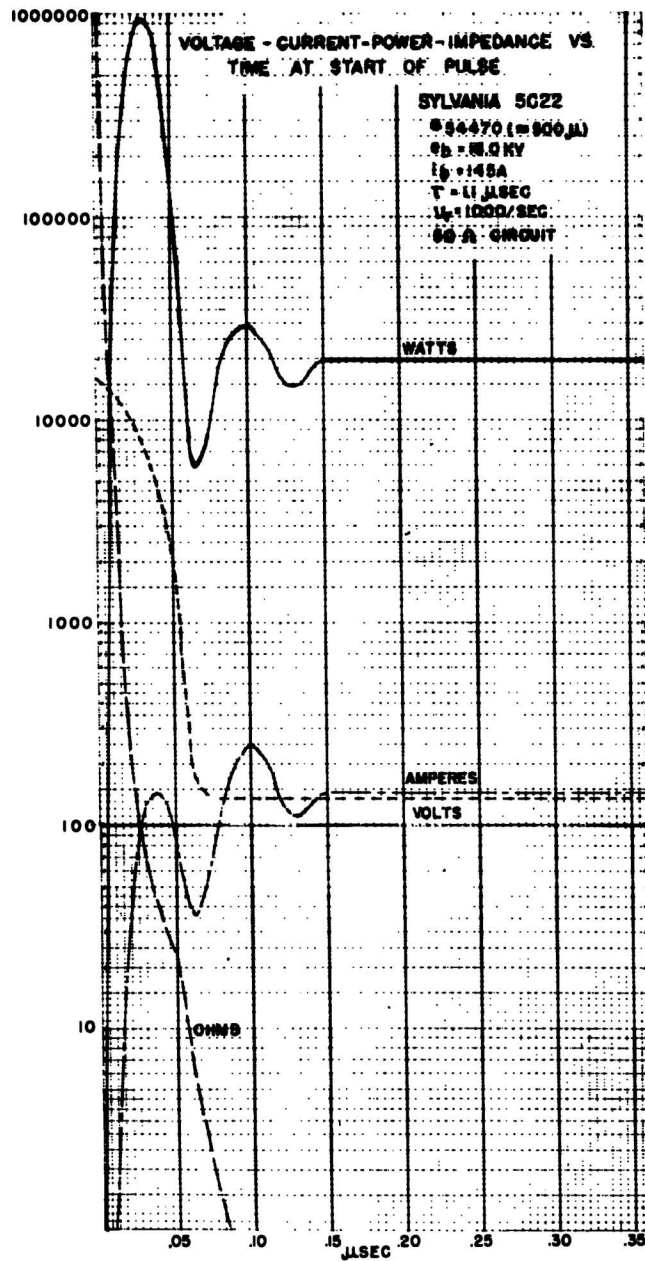


FIGURE 26b

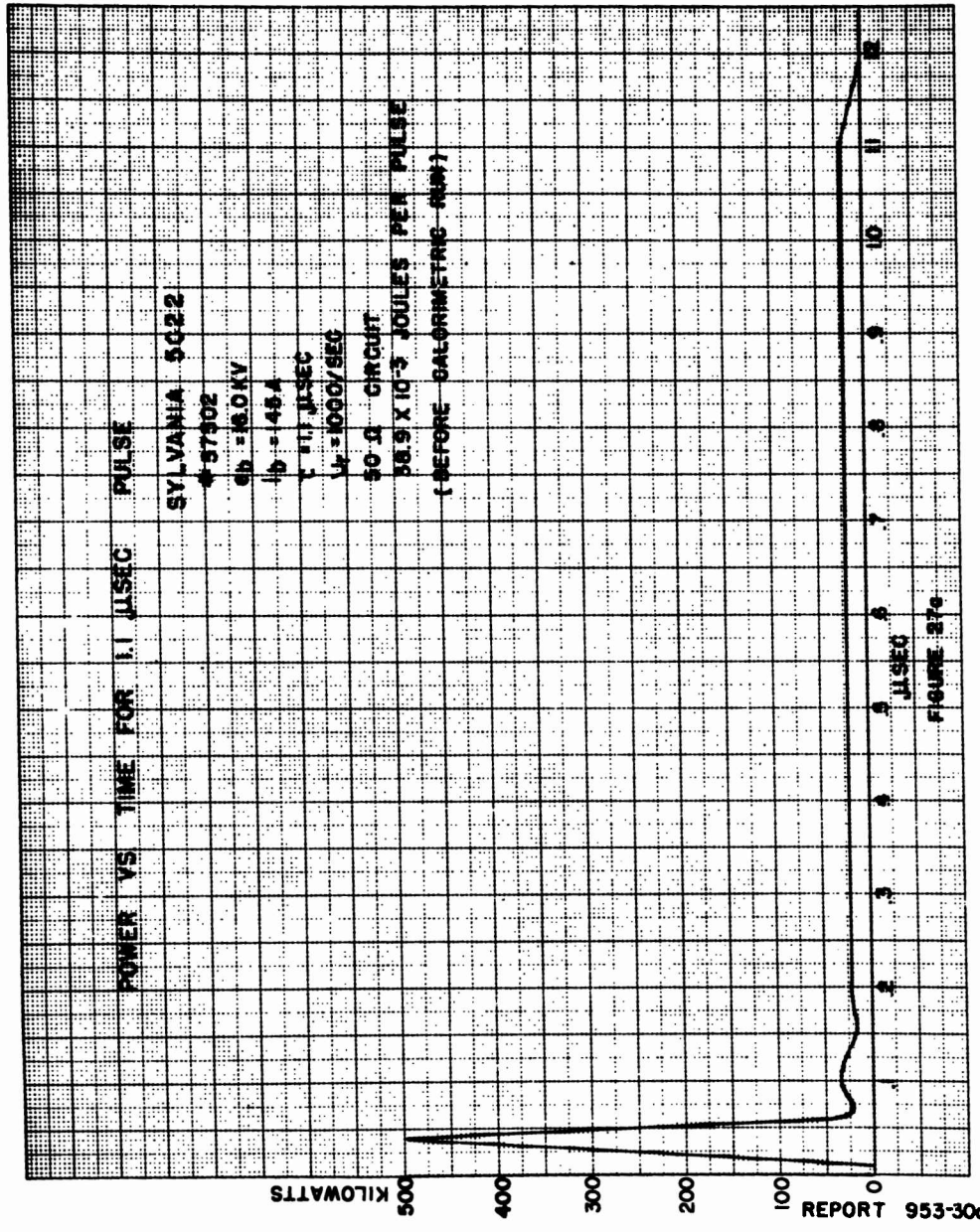


FIGURE 37c

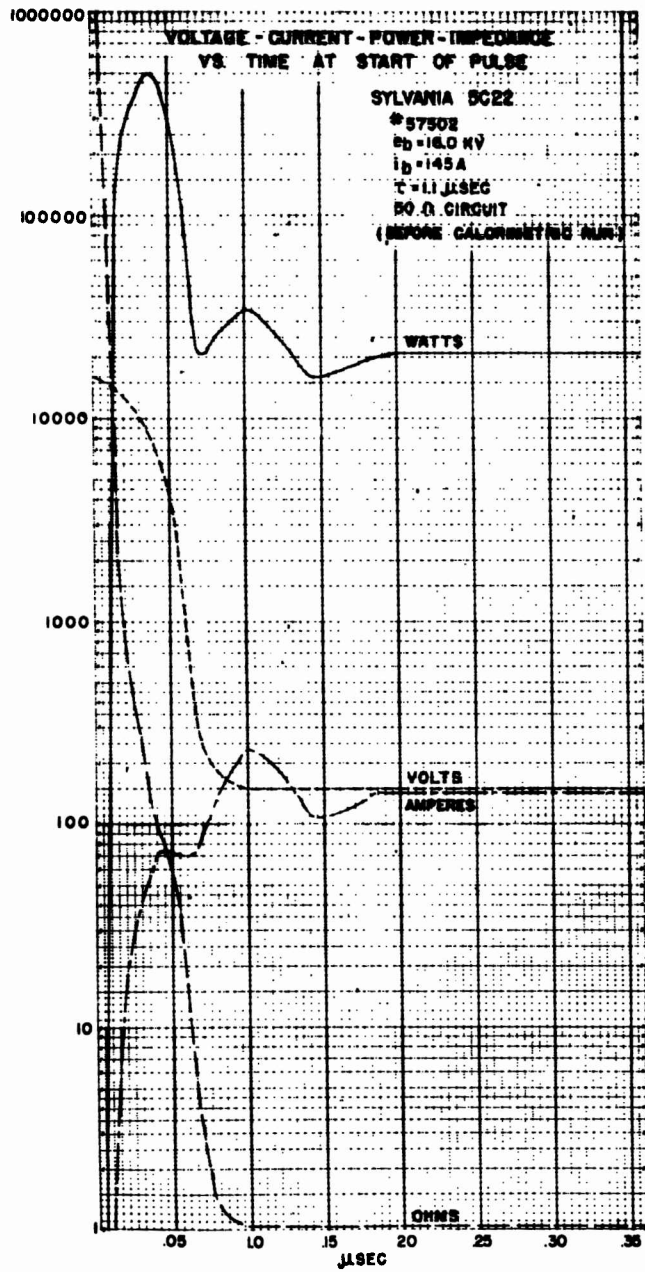
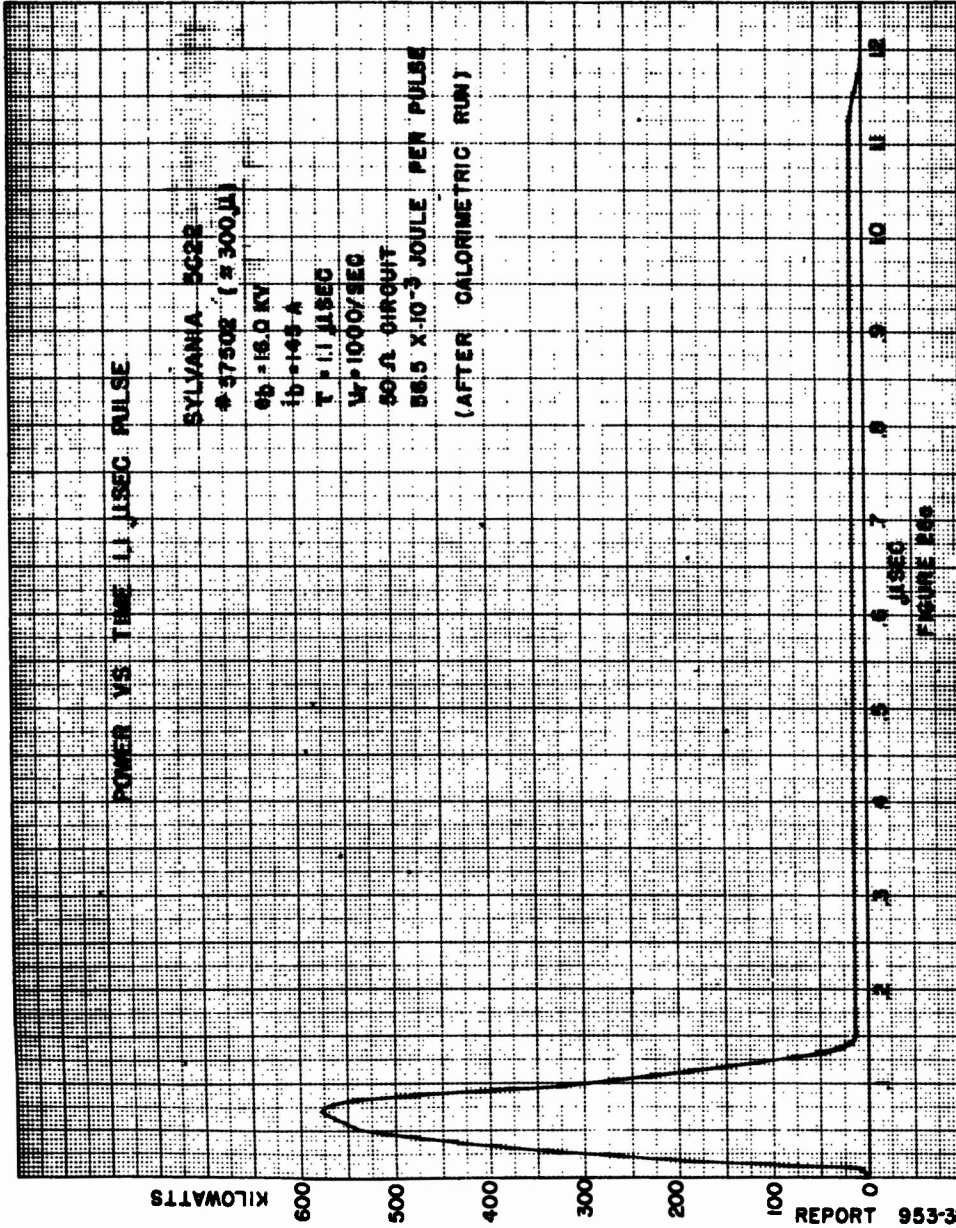


FIGURE 27b

REPORT 953-30b



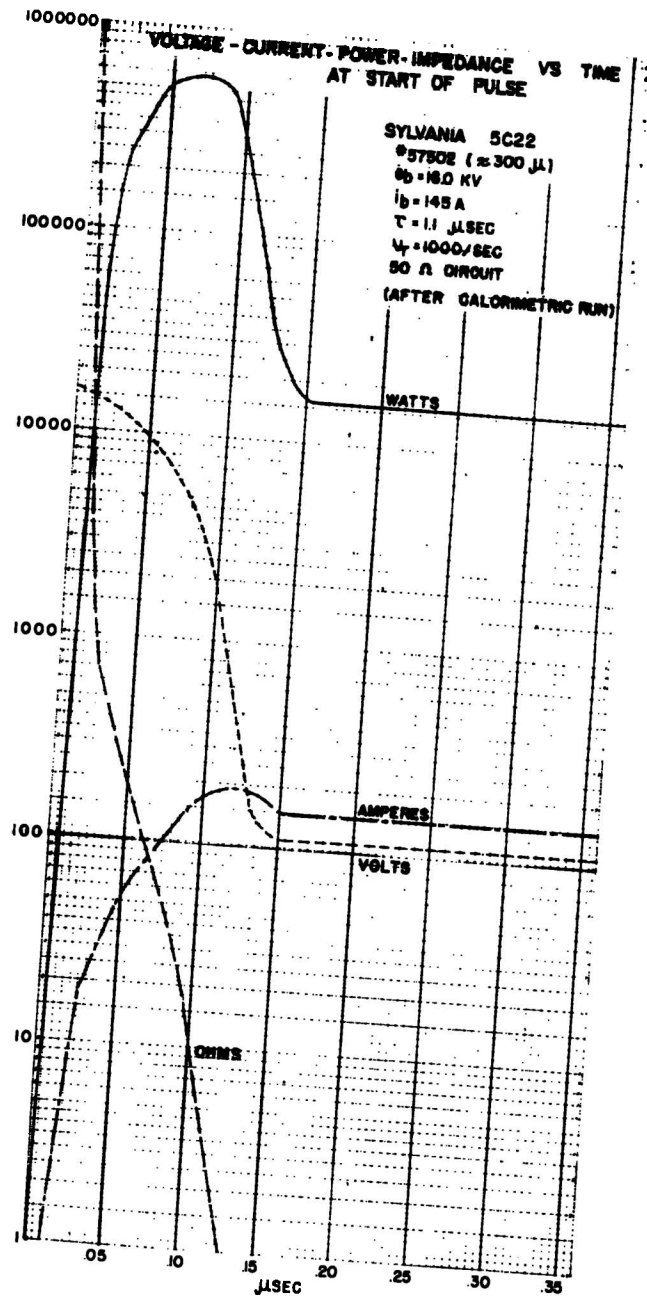


FIGURE 28 b

REPORT 953-31 b

These graphs were plotted for the two tubes in sections II and III. Figures 22 and 23 compare the 4035 and 5022 tubes at 1.1 μ sec pulse duration, and Figures 24, 25, and 26 show the variation in joules per pulse with operating power level for a 4035 in a 50 ohm circuit. Figures 22, 23, and 26 compare the 4035 and 5022 under conditions of equal pulse length and repetition frequency at their respective anode voltage and current ratings in a 50 ohm circuit.

In Figures 22a and 23a, for a 4035 operating at 1.1 μ sec duration, approximately 20-25% of the dissipated energy is used in establishing conduction. From Figures 22b and 23b, it is seen that the tube impedance reaches a very low value, about one ohm, in 0.45 to 1.0 μ sec.

As the operating power level is reduced, Figures 24, 25, and 26, the power vs time curve keeps its same general characteristic. In Figure 25a, with an anode voltage of 2.0 kv, 25% of the energy is used in establishing conduction, and this is the same fraction as at 8.0 kv.

In Figure 26a, for a typical sample of the 5022 at 16.0 kv, the energy dissipated in the tube per pulse for a 1.1 μ sec pulse is 42.7×10^{-3} joules as compared to approximately 13×10^{-3} joules for a 4035 at 8.0 kv and the same pulse length. Also, for the 5022, about 55% of the dissipated energy is lost in establishing conduction as compared to about 25% for the 4035.

Figures 27 and 28 show the effect of gas pressure on the distribution of dissipated energy during the pulse. This particular tube was faulty because in a few hours operation in a calorimeter, the gas pressure fell very rapidly and changed the characteristics of the tube. However, this case is a very interesting one and is a good illustration of the problem. In Figure 27, about 41% of the dissipated energy is used in establishing conduction, and the impedance is down to one ohm in about 0.2 μ sec. In Figure 28, about 71.5% of the dissipated energy is lost in establishing conduction, and the impedance is down to about one ohm in 0.17 μ sec.

B. Average Power Dissipation versus Pulse Repetition Frequency

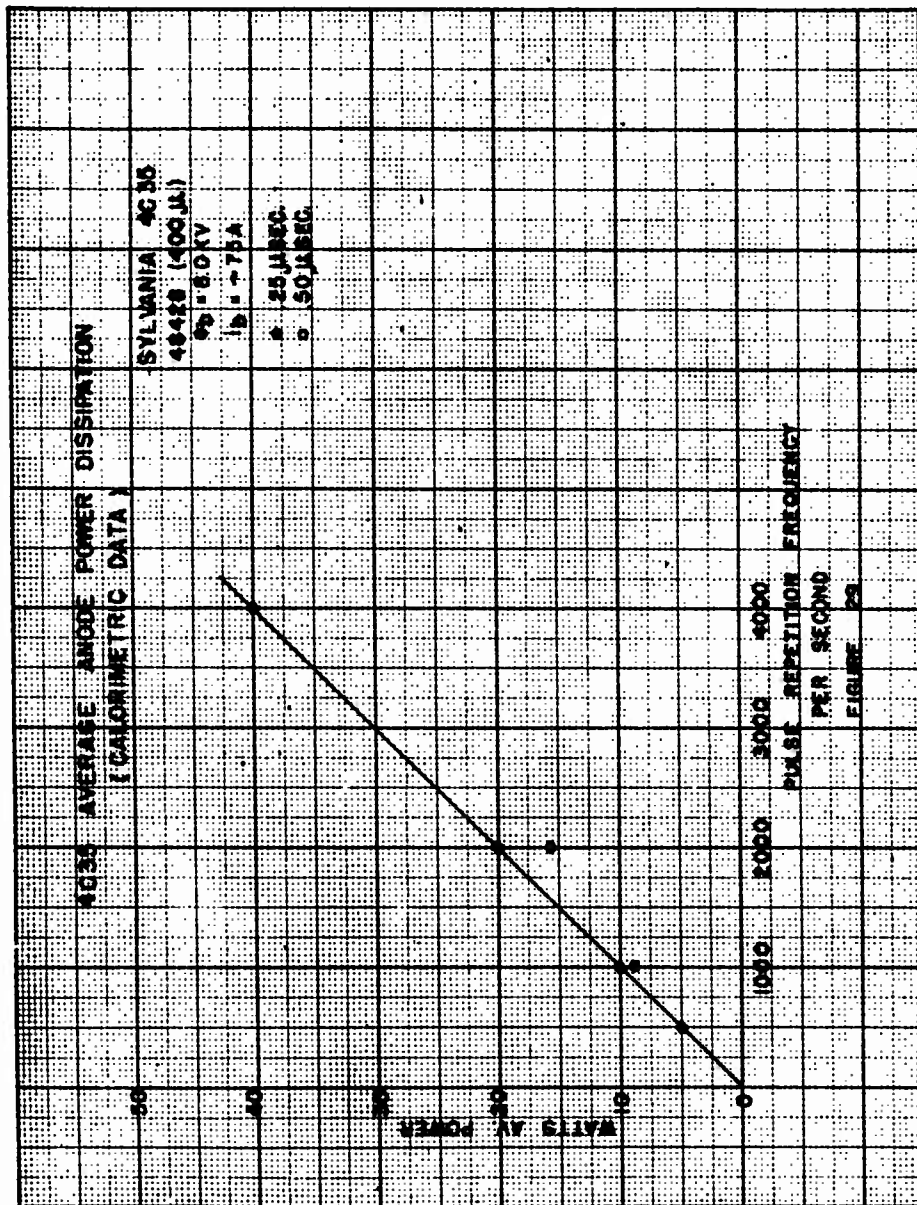
In Figure 29 is plotted the variation in average power dissipation with pulse repetition frequency. The variation is approximately linear, and since the average power is a function of pulse repetition frequency,

$$\text{watts} = (\text{joules/pulse}) (\text{pulses/second}),$$

the graph starts at the origin for zero prf.

C. Average Power Dissipation versus Pulse Duration

In Figure 30 is plotted the variation in average power dissipation with pulse duration. Theoretically, the intercept of these curves at zero pulse



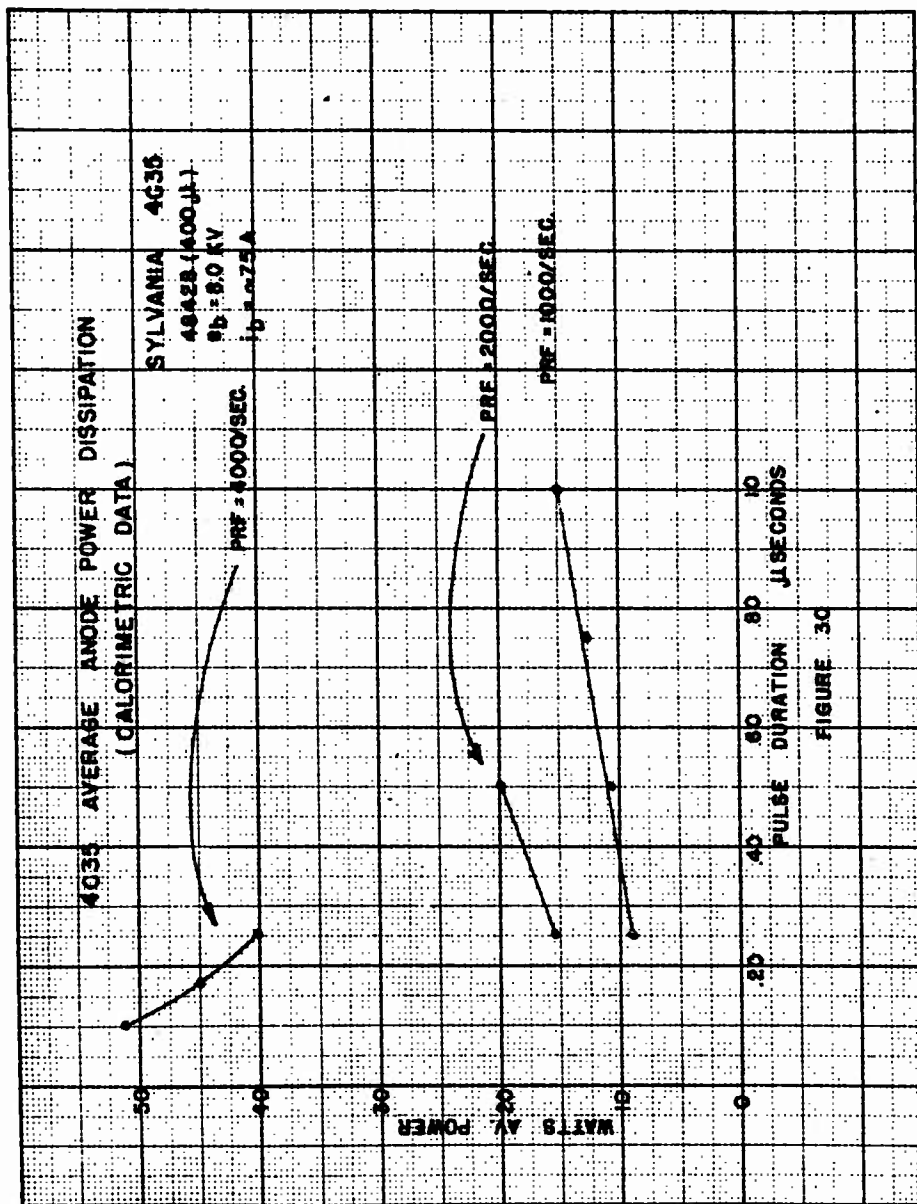


FIGURE 30

duration divided by the pulse repetition frequency should be equal to the energy dissipated in establishing conduction. However, this energy depends on the rate of rise of current and it has been already shown in Figures 3-8 that with the conventional Type B pulse forming networks, it is difficult to

keep $\frac{dib}{dt}$ constant for different pulse lengths. This practical difficulty

probably explains why the curves for 500/sec prf slope up instead of down with decreasing pulse length. It is probable that at pulse lengths less than

0.25 μ sec, the increase in $\frac{dib}{dt}$ more than compensated for the decrease in pulse

length. In any event, the tube becomes less efficient at short pulses with conventional pulse forming networks.

D. Average Power Dissipation versus Power Level

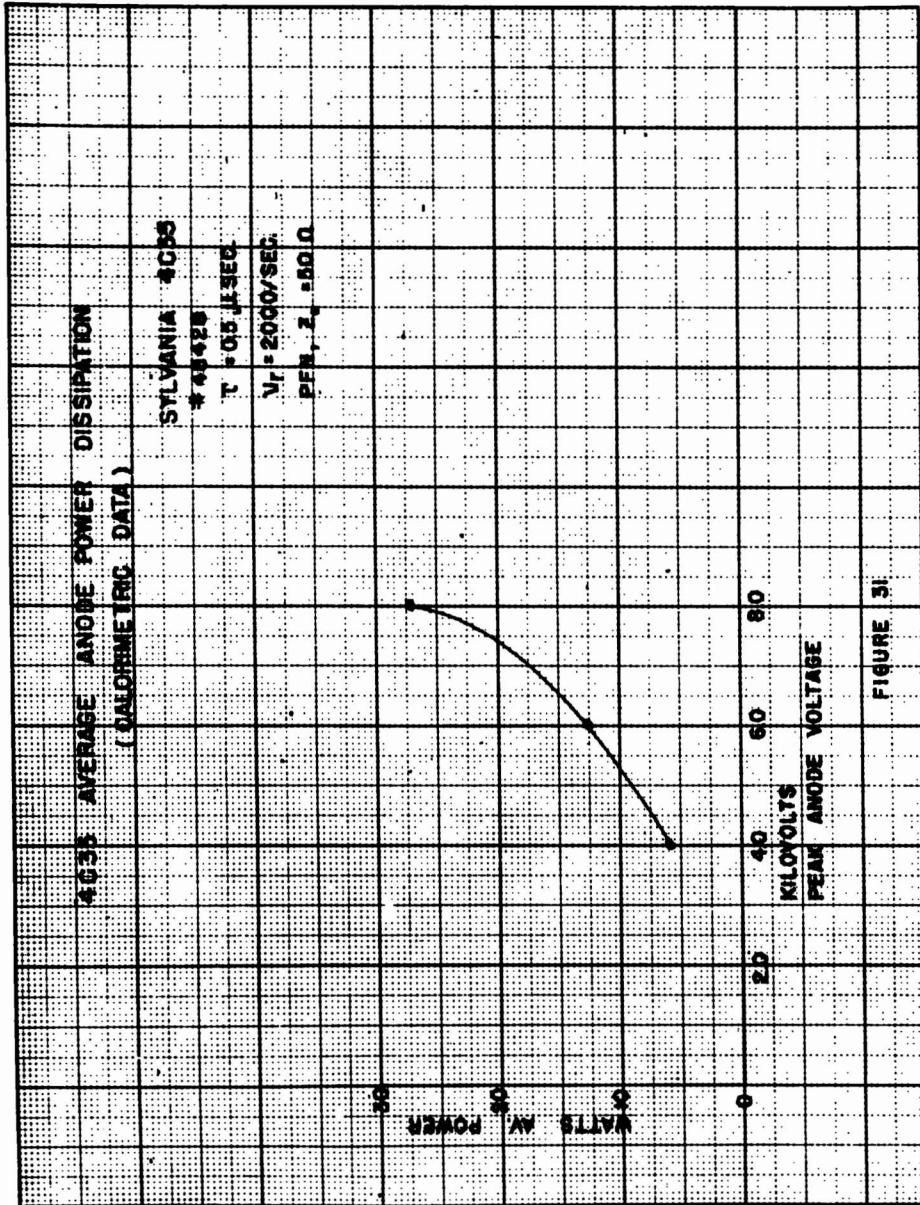
In Figure 31 is shown the variation in average power dissipation when the operating power level is reduced at constant circuit impedance. In Figure 32, the power was reduced by increasing the circuit impedance so that the anode voltage was kept constant while the peak current was varied. In Figure 33, the anode voltage was varied while the current remained approximately constant. The data of Figures 32 and 33 were taken by connecting pulse forming networks in series and parallel. These data show that if it is necessary to reduce average power dissipation in a thyratron by reducing the operating power level, it is more effective to reduce both current and voltage than just one or the other.

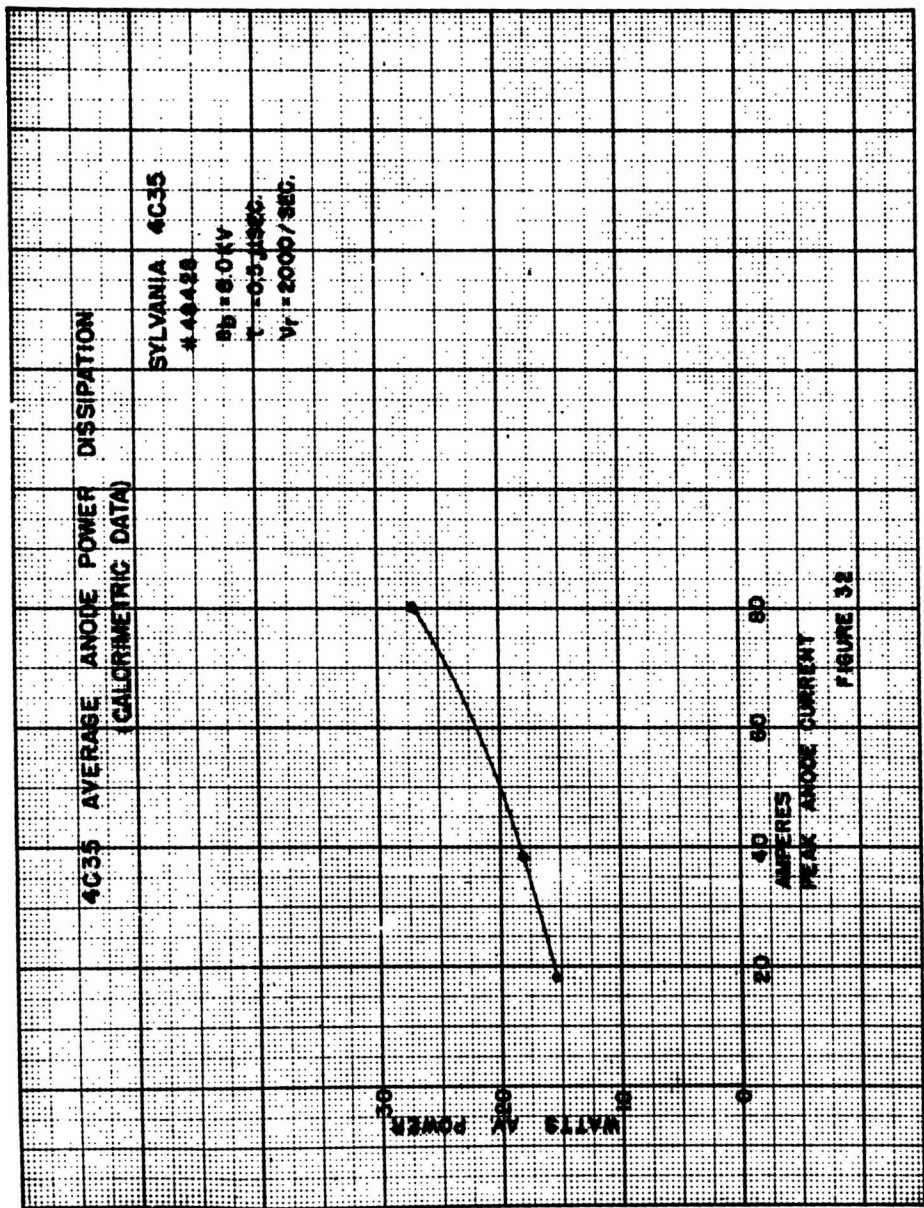
E. Average Power Dissipation as a Function of Pulse Repetition Frequency for Constant Duty

Figures 34, 35, 36, and 37 present data on four tubes. Since previous data have shown that $\frac{dib}{dt}$ tends to increase with shorter pulses with conven-

tional pulse forming networks, the curves of average dissipation versus prf for constant duty should not be linear. The linearity of the curves in Figures 34 and 35 is probably coincidence, and the non-linearity of Figures 36 and 37 is more correct. Figure 38 is a composite plot of Figures 34-37, and it is evident here that the average power dissipation increases with decreasing gas pressure. This may be due to the increase in energy dissipated in establishing conduction as shown in Figures 27 and 28. Figure 39 is a plot for a 5022 thyratron. The effect of series anode inductance on dissipation can be seen here. It was shown in Figure 12 that series inductance reduced

$\frac{dib}{dt}$. By limiting $\frac{dib}{dt}$, the energy dissipated during the start of conduction is reduced, and the average anode power dissipation is lowered. The reduction





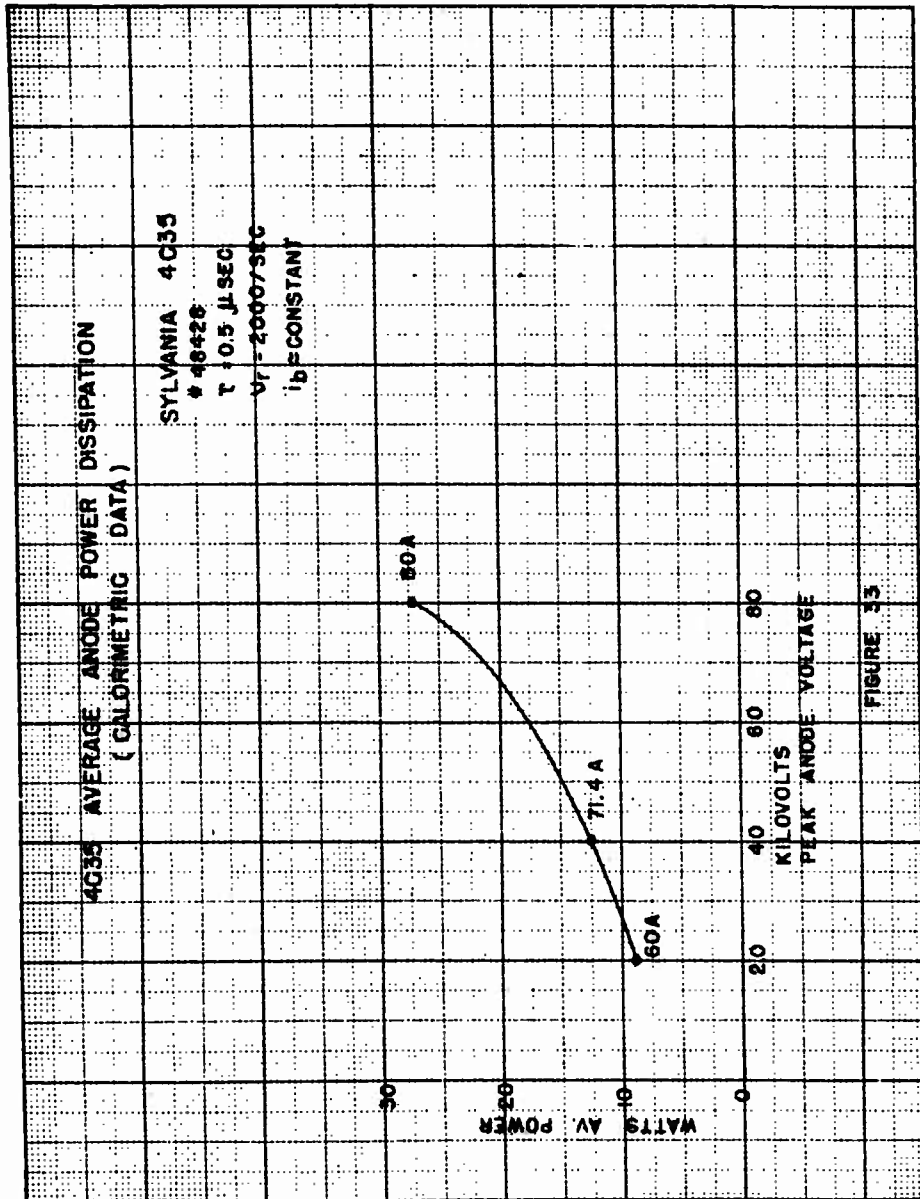
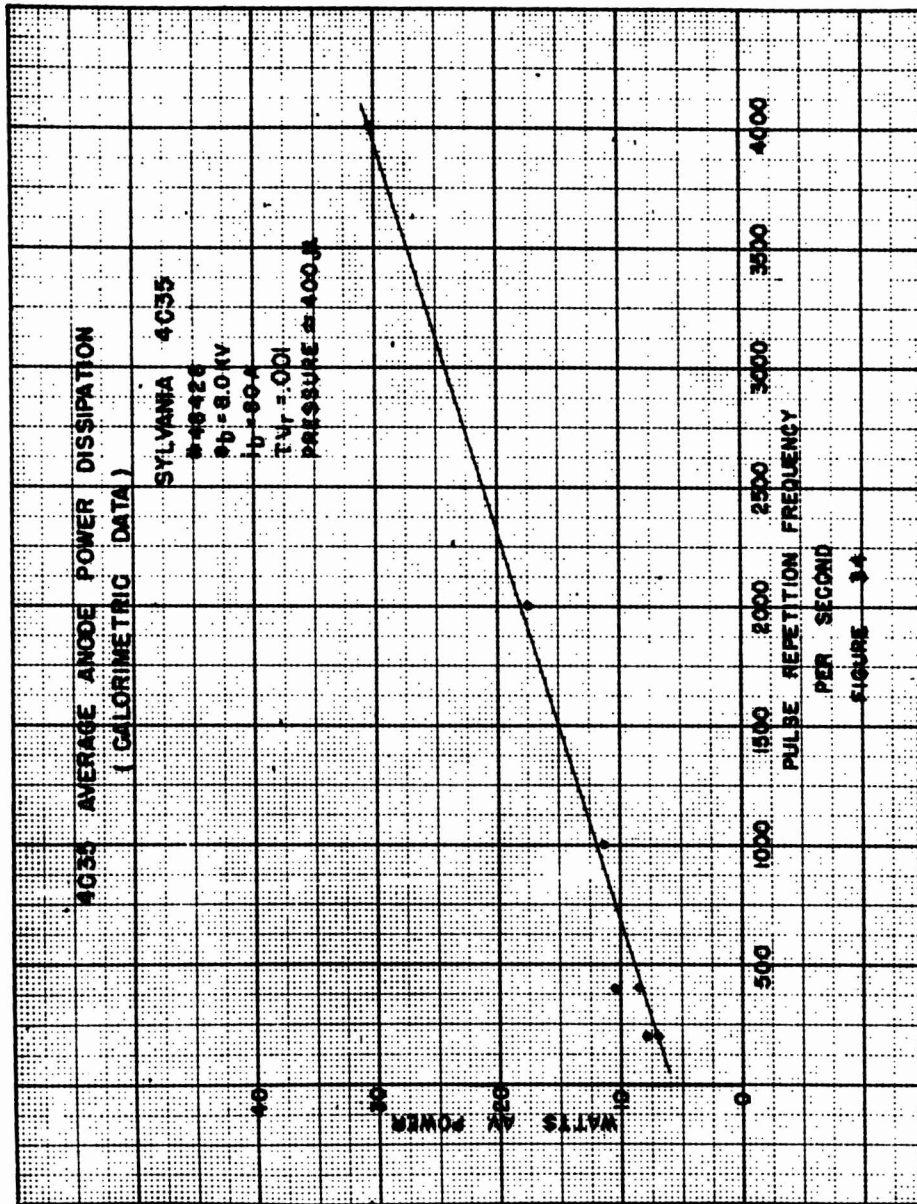
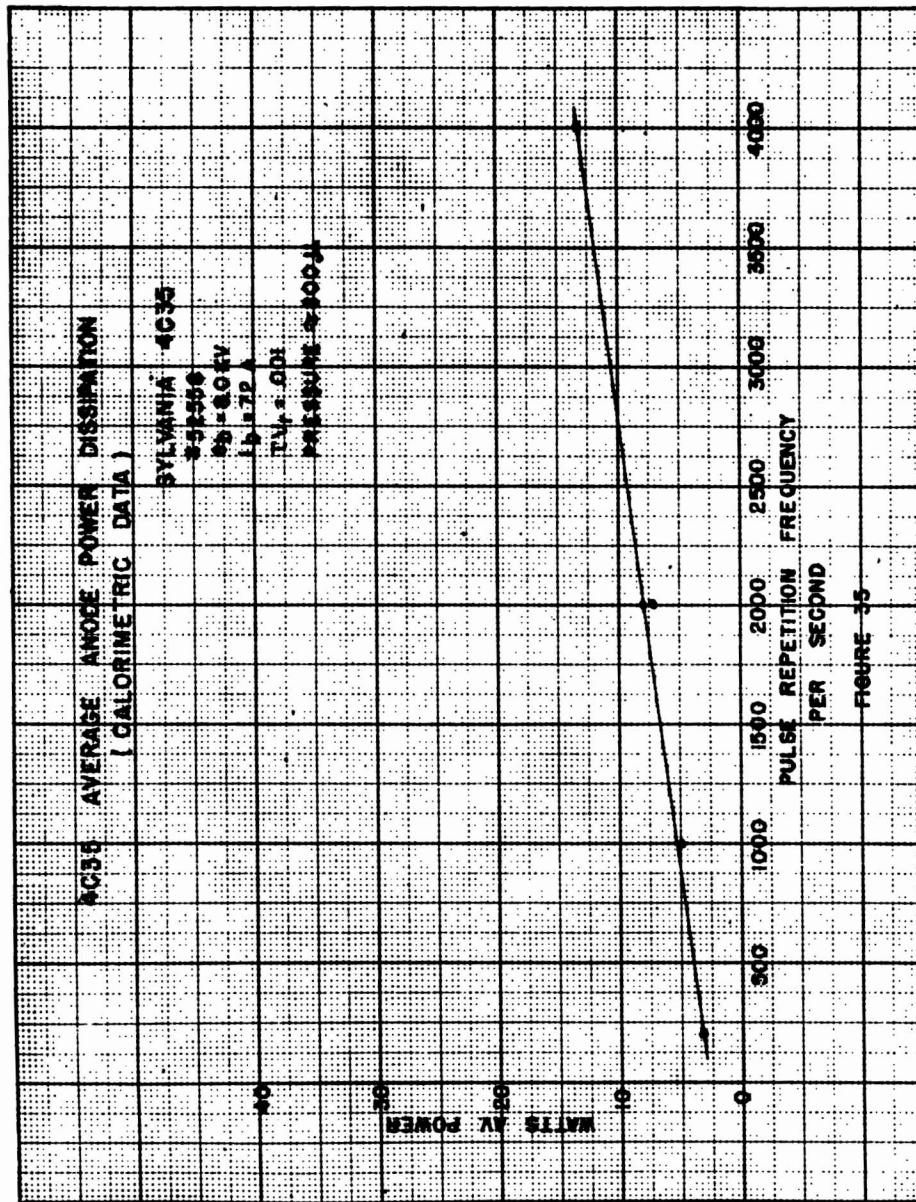


FIGURE 33

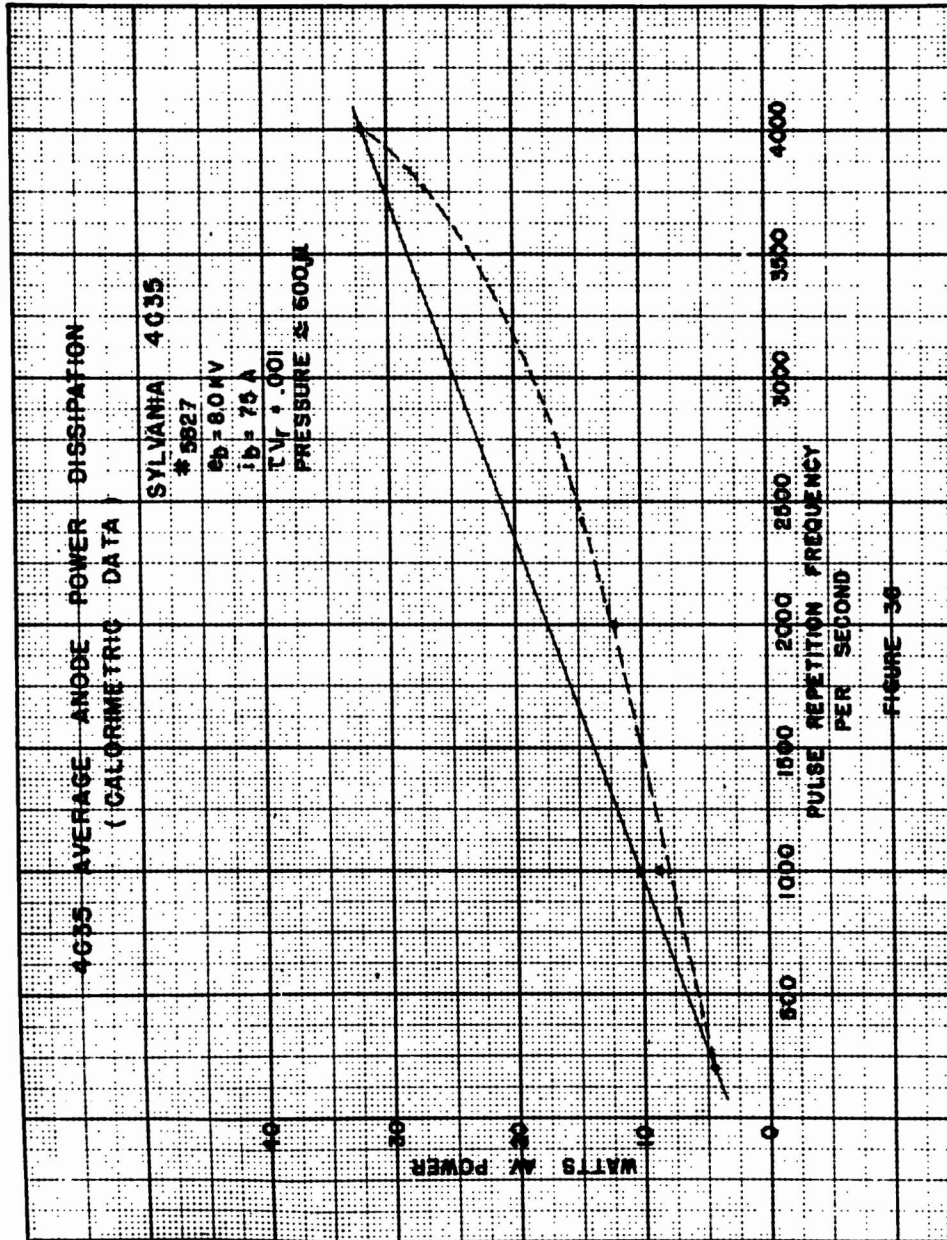


REPORT 953-39

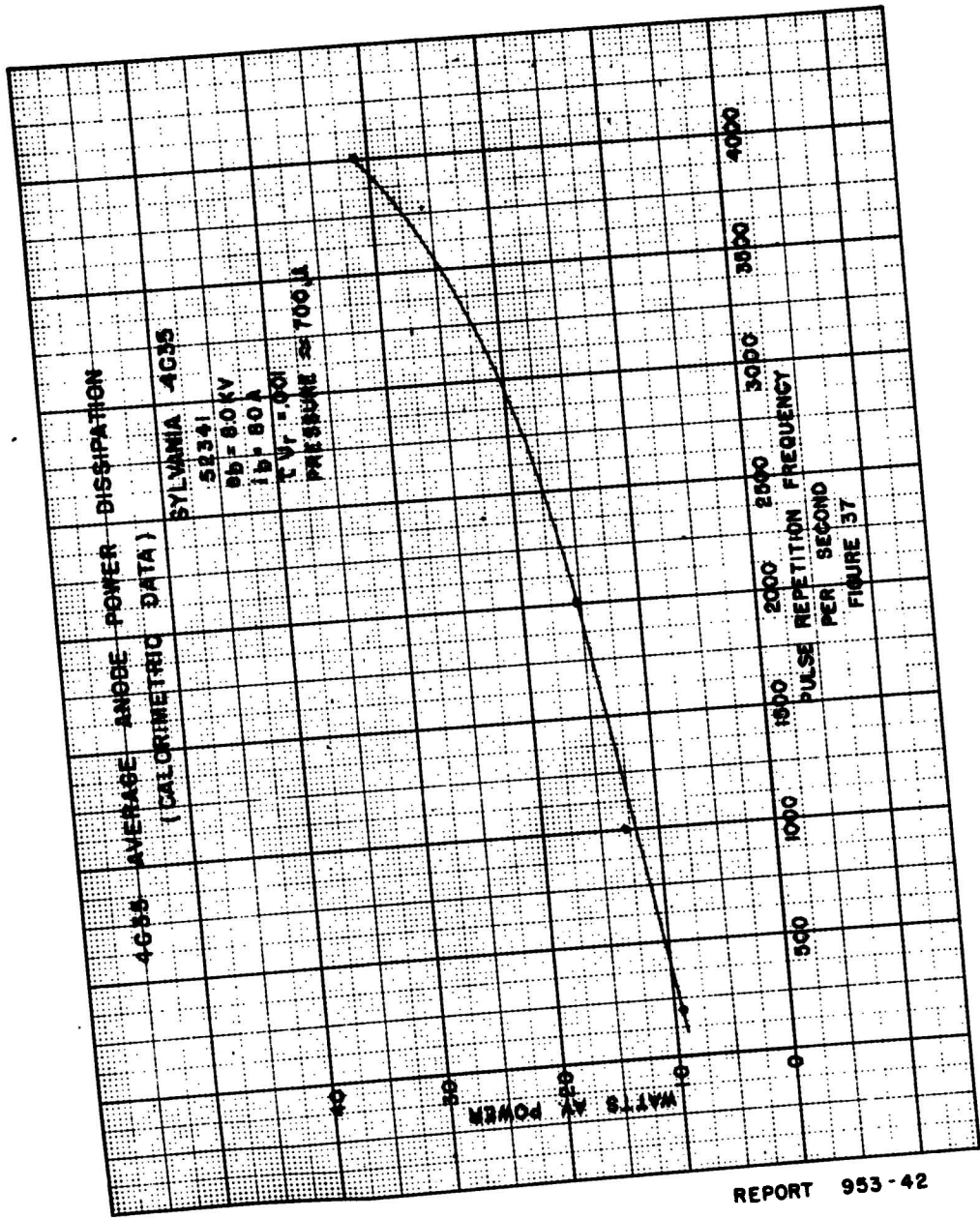


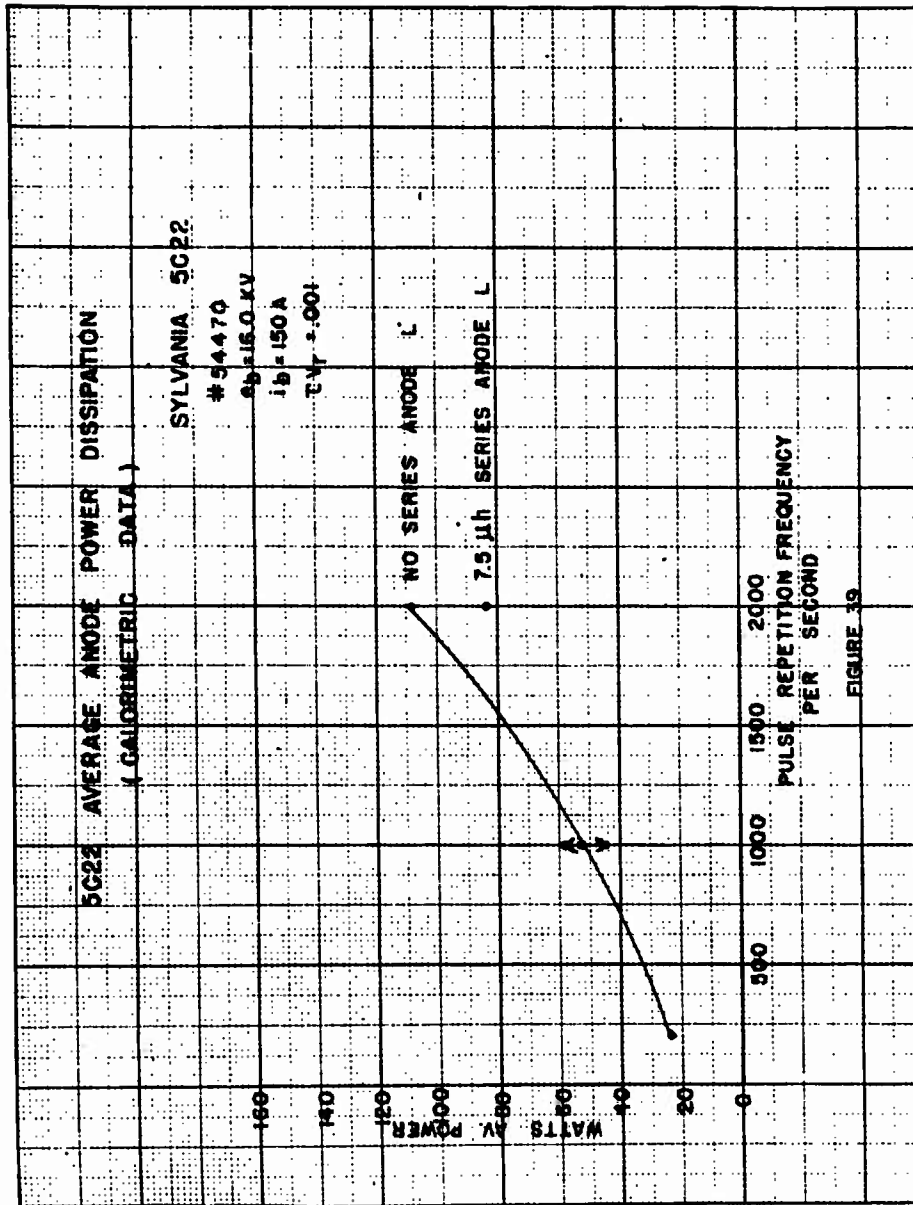
REPORT 953-40

FIGURE 35



REPORT 953-41





REPORT 953-44

of average power dissipation by the use of series inductance, and the increase of average power dissipation by the use of tube shield capacity across the thyatron have been verified by life tests.

F. Comparison of calorimetric data and V-I data for 1 μ sec pulse, 1000/sec., out a 50 ohm circuit.

<u>Tube</u>	<u>E_b</u>	<u>Calorimeter</u>	<u>V-I</u>
52441	4.7 kv	17.7 watts	15.9 watts
48428	5.0	11.9	9.8
5827	5.2	9.0	11.0
54470	15.0	52.0	42.7
57411	16.0	53.6	-
57765	15.0	47.6	-

*These data were the first taken on these tubes. All the other data were taken after this tube had been operated considerably, and the reason for the increase in dissipation in all the other curves is probably due to fluctuations in gas pressure.

To a fair approximation, the 5022 must dissipate approximately four times the energy that the 4028 dissipates when the two tubes are operated at their respective maximum ratings, and the same pulse duration and repetition frequency.

The data presented in this report indicate that the energy dissipated in the hydrogen thyatron depends on the following:

1. e_b -- anode voltage at the start of conduction.
2. i_b -- peak anode current.
3. pulse duration.
4. gas pressure -- controls $\frac{de_b}{dt}$ and to some extent $\frac{di_b}{dt}$.
5. cathode emission -- controls tube drop.
6. $\frac{di_b}{dt}$

With this number of possible variables affecting dissipation, particularly gas pressure and cathode emission, it is almost impossible to duplicate data from one time to another with any degree of accuracy.

The writer wishes to acknowledge the assistance of John T. Downing, Leo Shore, and Miss Maribel Carter in obtaining the data on which this report is based.

Stanley J. Krulikowski, Jr.
November 27, 1945

RFFL - C

4 8 5

A.T.I.

1 3 8 6 0

Kralikoski, S.

DIVISION: Electronics (3)

SECTION: Electronic Tubes (8)

CROSS REFERENCES: Thyratrons (94180); Tubes, Electronic (95220)

AD-381579

ATI- 13860

ORIG. AGENCY NUMBER

R-953

DIVISION

AUTHOR(S)

AMER. TITLE: Hydrogen thyratrons in pulse generator circuits

FORG'N. TITLE:

ORIGINATING AGENCY: Massachusetts Inst. of Technology, Radiation Lab., Cambridge

TRANSLATION:

COUNTRY	LANGUAGE	FORG'N. CLASS.	U. S. CLASS.	DATE	PAGES	ILLUS.	FEATURES
U.S.	Eng.		Unclass.	Mar '46	55	46	graphs

ABSTRACT

Data are presented on the operating characteristics of hydrogen thyratrons in line-type pulse generator circuits. The rate of fall of anode voltage, rate of rise of anode current, and tube drop are presented. In addition to the operating anode voltage and current, the most important parameter governing tube dissipation is gas pressure. This is demonstrated both calorimetrically and by V-I plot. Because of the great number of possible variables that govern tube dissipation, most of them uncontrollable, it is impossible to reproduce data with any degree of accuracy.